

Responses to referee #3 and short comment #1 on “Detection of critical PM<sub>2.5</sub> emission sources and their contributions to a heavy haze episode in Beijing, China, using an adjoint model” **and marked-up version of the manuscript.**

## To Referee #3

Dear referee,

Thank you very much for your valuable comments. Revisions in the track change version of the manuscript are in red or shaded. This document is organized as follows: the referee’s comments are in black and responses to the comments are in blue.

### 1. Overview

The manuscript by Zhai et al. investigates sources of PM<sub>2.5</sub> for a pollution episode in Beijing using adjoint modeling. The work is a nice start, and a good use of the new tools that this group has developed. However, the manuscript overall feels a bit premature; it reads like a first draft. The overall purpose of using the adjoint model is not well articulated, nor is the tool used to its full potential. The comparisons and evaluations to observations and other studies are often qualitative and not particularly well fleshed out, and the presentation of results is murky in a few critical areas. The manuscript also requires substantial grammatical editing throughout. It is possible the work would be suitable for ACP after major revisions, but a different journal such as Atmospheric Research may be a better fit.

Response: Thank you very much for your comments. This study selected the same pollution episode as that in a previous work (Zhai et al., 2016) carried out by our group. In contrast to the previous work, the overall purpose of using the **backward** adjoint model is to provide detailed temporal-spatial variation of PM<sub>2.5</sub> critical sources with high computational efficiency, which is almost infeasible to be obtained through the **forward** emissions off-and-on sensitivity analysis (the perturbation approach) due to high computational cost. This overall purpose is then added in the **introduction**. To take better advantage of the adjoint model, we then divided emission sources impacts on Beijing PM<sub>2.5</sub> into different provinces around Beijing (added in section 4.4). In addition, model evaluations are strengthened in section 3.3 with measurements from two more observational sites (one rural station and one urban station) and qualitative statistical metrics of model performance are added. The whole manuscript is edited by the Enago (<http://www.enago.com>) English editing services and verified by the authors. The authors will also order the English copy-editing services from Copernicus.

### 2. Major comments

- 2.10-14: While it is true that an adjoint model provides more precise estimates of the sensitivity (partial derivative), this in some cases may also be viewed as a downside compared to perturbation approaches when performing sensitivity calculations for the purpose of source attribution, since the adjoint model fails to capture the nonlinear response of atmospheric chemistry to **substantial changes** in emissions. Overall, the topic of how these types of sensitivities are interpreted for source contributions needs to be directly addressed in the introduction and methods, and expanded upon in the interpretation of results in more detail.

Response: Thank you very much for your valuable comments. We have made the corresponding revisions in the introduction, methods and interpretation of results. The revised presentation **emphasized** that the adjoint sensitivity reveals the changes in concentration due to small perturbations in emissions sources, in other words, the adjoint model estimates the incremental influence of specific sources on air quality attainment. Corresponding revisions are green shaded.

- Introduction: Several previous studies of source contributions to PM<sub>2.5</sub> in Beijing are mentioned, but

they are only discussed in terms of their computational methods. That would be fine if this paper was in G.M.D. and strictly a discussion of methods. But for a scientific paper in ACP, the authors need to discuss the actual scientific findings of previous works. They need to clearly articulate what has previously been written about the sources that contribute to Beijing PM<sub>2.5</sub>, and how their current study will advance the understanding of sources (most likely by providing insights into the spatial variability of contributions that can be most readily obtained using adjoint methods). Some justification for studying the specific pollution episode of Nov 19-21, 2012, also needs to be provided.

Response: Following the referee's comments, we have deleted the paragraph that describes current applications of adjoint modeling in atmospheric chemistry and added new information to discuss the actual scientific findings of previous works regarding sources that contribute to Beijing PM<sub>2.5</sub>. We then illustrated previous studies that implement the adjoint model in Beijing air pollutants tracking, which proved the high efficiency and accuracy of an atmospheric chemistry adjoint model in Beijing air pollutants source apportionment. Thereafter, justification for studying the Nov 19-21, 2012 pollution episode is provided. In the end, we point out that our work advances the understanding of Beijing PM<sub>2.5</sub> sources by providing insights into the spatial and temporal variability of emission source contributions from each of the surrounding provinces as well as from local and environs transports. Revisions are in red or shaded in the manuscript.

- 5.26: The authors claim that the initial concentrations and boundary conditions are set as the “observed monthly means”, but this does not make sense, as it is impossible that the concentrations of all species were observed at all locations throughout the domain in order to establish an observationally-derived initial condition and boundary condition. Thus, please describe in more detail how initial and boundary conditions are estimated.

Response: Thank you very much for pointing this incorrect presentation out. Here the initial and boundary values for O<sub>3</sub> and OH radical were taken from climatic means, and zeros for each aerosol species (Zhou et al., 2012). Revisions in section 3.3 are in red in the first paragraph.

Hope it is reasonable now.

- Section 3: Please include an entire new section covering in detail the emissions (anthropogenic and natural) used in this model, including a description of their daily and hourly variability. These are critical for understanding the significance of sensitivities of the form  $\frac{\partial J}{\partial S_n} S_n$ .

Response: Thank you very much for your comments. Detailed description of emissions used in this model is added in the second paragraph of section 3.3 (red and underlined in the manuscript). Gridded distribution of overall PM<sub>2.5</sub> primary emission sources is illustrated in Fig. 2, and the hourly variability of the overall particle sources (as well as sulphate as an example) in Beijing is shown in Fig. 3. Description of Fig. 2 and Fig. 3 are added in the third paragraph in section 3.3 (red and underlined in the manuscript).

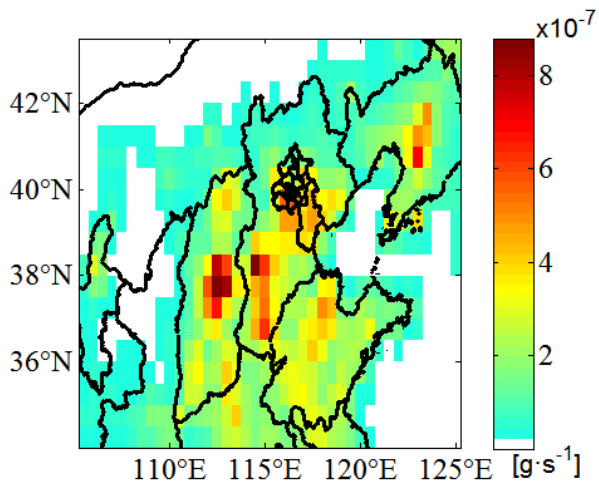


Figure 2. Gridded distribution of PM<sub>2.5</sub> primary emission sources.

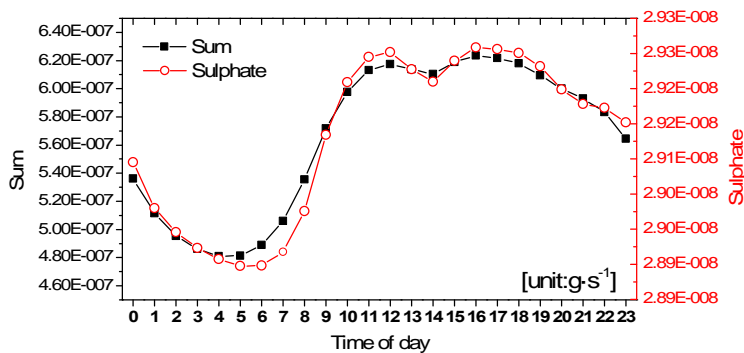


Figure 3. Hourly variation of primary PM<sub>2.5</sub> emission sources in Beijing.

• Fig 3(a) Section 3.3: The discussion model performance evaluation needs to be improved and expanded. It appears that the simulation over-estimates PM<sub>2.5</sub> concentrations, although the timing of the peaks is well-correlated with the measurements. Are there no measurements on Beijing site to compare with? Are only measurements of total PM<sub>2.5</sub> available? How well does this model do at reproducing concentrations of specific aerosol components, such as BC, sulfate, nitrate, etc.? If this has been documented in previous work for Beijing specifically, then the authors should be more quantitative when discussing the model skill using metrics such as normalized mean bias, normalized mean error, etc. It is also interesting that the model over-estimates measurements, given that many air quality models fail to represent the high levels of PM<sub>2.5</sub> concentrations observed during peak episodes in Beijing owing to missing treatment of heterogenous chemistry, as described in several recent papers such as Wang et al. (PNAS, 2016, doi:10.1073/pnas.1616540113) and Cheng et al. (Science Advances, 2016, doi:10.1126/sciadv.1601530).

Response: The hourly PM<sub>2.5</sub> concentration measurements at Guanyuan (GY), an urban site, and Dingling (DL), a rural observation site, are added to evaluate the model performance. Meanwhile, the performance statistics including correlation coefficient (R), mean bias (MB), normalized mean bias (NMB), normalized mean error (NME), mean fractional bias (MFB) and mean fractional error (MFE) are also listed in Table 1 and accordingly analyzed in the context in red. We didn't obtain the available measurements for specific aerosol components. The GRAPES-CUACE modeling system is an on-line coupled meteorology-chemistry modeling system which adopts the size-segregated multicomponent aerosol algorithm in its aerosol module. Except for ammonium, sulphates, BC, OC, sand/dust, nitrates and sea salts are segregated into 12 size bins. Therefore, it has better performance in simulating aerosol concentrations.

Revisions in the manuscript:

- ① Model performance discussions are in red in section 3.3.
- ② Locations of GY and DL stations are added in Figure 4:

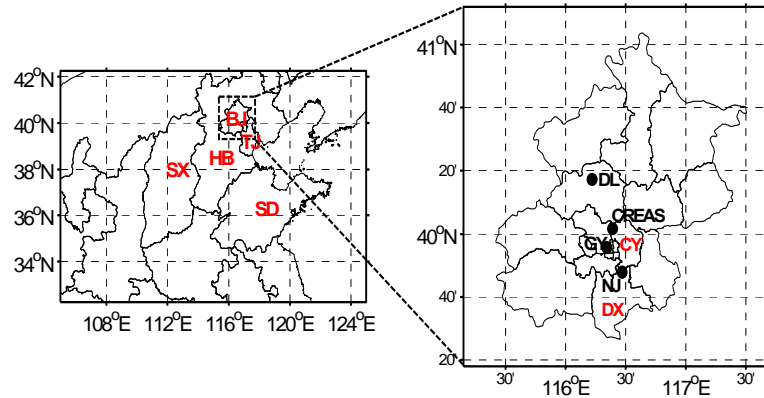


Figure 4. Left: Model domain settings and location of Beijing municipality (BJ), Tianjin municipality (TJ), Hebei province (HB), Shandong province (SD) and Shanxi province (SX); right: Locations of the Chinese Research Academy of Environmental Sciences (CREAS) station, the Guanyuan (GY) station, the Dingling (DL) station, the Nanjiao (NJ) station, Daxing district (DX) and Chaoyang (CY) district.

- ③ Hourly concentration curves at GY and DL stations are added in Figure 5b and 5c:

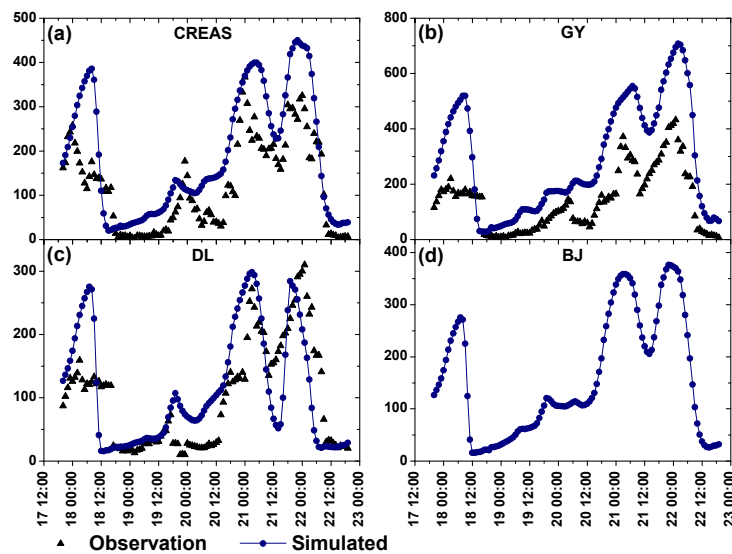


Figure 5. (a)-(c): Comparisons of the observed (black solid triangles) and simulated (blue dot-line) hourly  $PM_{2.5}$  concentrations at Chinese Research Academy of Environmental Sciences (CREAS) station, Guanyuan (GY) station and Dingling (DL) station; (b): Hourly variations of average  $PM_{2.5}$  concentration over Beijing municipality.

- ④ Statistic metrics are listed in Table 1:

Table 1 Performance statistics of  $PM_{2.5}$  concentration.

Simulated Time Period	Stations	Obs. ( $\mu\text{g}\cdot\text{m}^{-3}$ )	Sim. ( $\mu\text{g}\cdot\text{m}^{-3}$ )	R	MB ( $\mu\text{g}\cdot\text{m}^{-3}$ )	NMB (%)	NME (%)	MFB (%)	MFE (%)
20:00 Nov. 17-22, 2012	CREAS	121.5	190.9	0.87	69.4	57.2	185.2	53.6	60.1
	GY	139.0	289.4	0.91	150.4	108.1	183.3	65.2	68.3
	DL	101.4	112.2	0.69	10.8	10.7	85.6	15.6	39.6

Notes: Mean bias:  $MB = \frac{1}{n} \sum_{i=1}^n (Sim_i - Obs_i)$ ;

Normalized mean bias:  $NMB = \frac{\sum_{i=1}^N (Sim_i - Obs_i)}{\sum_{i=1}^N Obs_i} \times 100\%$ ;

Normal mean error:  $NME = \frac{1}{n} \sum_{i=1}^n \frac{|Sim_i - Obs_i|}{Obs_i} \times 100\%$

Mean fractional bias:  $MFB = \frac{1}{N} \sum_{i=1}^N \frac{(Sim_i - Obs_i)}{(Obs_i + Sim_i/2)}$ ; Mean fractional error:  $MFE = \frac{1}{N} \sum_{i=1}^N \frac{|Sim_i - Obs_i|}{(Obs_i + Sim_i/2)}$

• Section 4.1: There are several species and sectors that have emissions that contribute to PM<sub>2.5</sub> formation. Which emissions are considered in the presentation of the results here? In other works, how is S<sub>n</sub> defined? Are anthropogenic and natural sources included? What type of anthropogenic sources? Is it the total emission across all species? This is an essential missing detail. The results have little scientific or policy relevance in current form, given that they are only presented in terms of local vs nonlocal sources (a point for which use of an adjoint model would be overkill).

Response: Thank you for pointing this vague presentation out.

In the forward model processes, the emissions in GRAPES-CUACE include both anthropogenic and natural sources. Anthropogenic sources are constructed by Cao et al. (2011) based on statistical data from government agencies for the year 2007. They are the hourly gridded off-line emissions intensity for 32 species including black carbon (BC), organic carbon (OC), sulphate, nitrate, fugitive dust particles, in addition to 27 gases. Emission source types include biomass combustion, residences, power generation, industry, transportation, livestock and poultry breeding, fertilizer use, waste disposal, solvent use, and light industrial product manufacture (Cao et al., 2011). Natural sources are calculated with the parameterizations of natural sea salt and natural sand/dust emissions in the model.

In the backward GRAPES-CUACE aerosol adjoint model, as CAM (Canadian Aerosol Model) contains major aerosol processes (generation, hygroscopic growth, coagulation, nucleation, condensation, dry deposition/sedimentation, below-cloud scavenging, aerosol activation and chemical transformation of sulphur species in clear air and in clouds) in the atmosphere, the GRAPES-CUACE aerosol adjoint model is capable of coupling major aerosol processes in the atmosphere into its simulations of the sensitivities of the objective function to primary aerosol sources. Therefore, S<sub>n</sub> in the adjoint sensitivity coefficients  $(\partial J / \partial S_n) \cdot S_n$  contains: black carbon (BC), organic carbon (OC), sulphate, nitrate, fugitive dust particles. Detailed description of emission sources and the definition of S<sub>n</sub> is added in section 3.2 & 3.3 (underlined in the manuscript). Spatial distribution and hourly variation of the primary PM<sub>2.5</sub> sources are also presented in section 3.3 (underlined in the manuscript).

To take advantage of the adjoint model, we subdivide local and nonlocal sources impacts into impacts from local Beijing and each surrounding province of Beijing: Beijing, Tianjin, Hebei, Shanxi and Shandong. A new section, section 4.4 is added to analyze the ‘sensitivity coefficients of surface PM<sub>2.5</sub> concentration peaks in Beijing to primary emission sources from local Beijing and each of the surrounding provinces (Figure 9)’. Section 4.4 is in red.

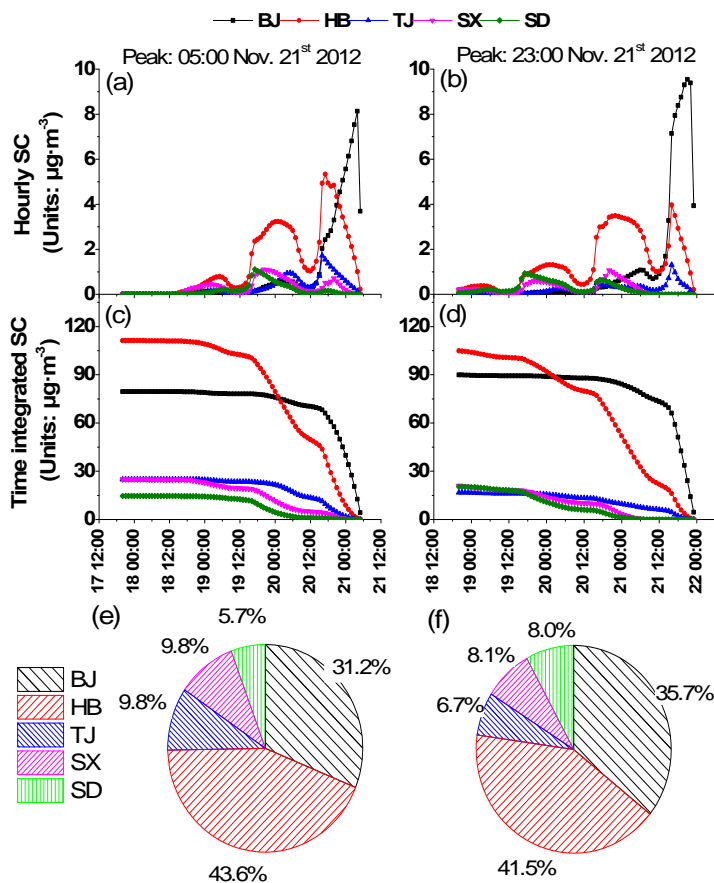


Figure 9. Sensitivity coefficients of surface PM<sub>2.5</sub> concentration peaks in Beijing to primary emission sources from local Beijing and each of the surrounding provinces. The left and right panels correspond to PM<sub>2.5</sub> concentration peaks at 05:00 LT and at 23:00 LT on 21 November 2012 respectively. (a–b) illustrate hourly instantaneous sensitivity coefficients to emission sources from local Beijing, Hebei province, Tianjin city, Shanxi province and Shandong province. (c–d) show the time-integrated sensitivity coefficients to local and surrounding provincial emission sources. (e–f) are the contribution ratios of emission sources from each surrounding province to PM<sub>2.5</sub> concentration peaks.

• 8.9-11: This statement hasn't really been demonstrated. To use the adjoint sensitivities to “reproduce” the air pollution episode, one would need multiply the time series of sensitivities by the time series of emissions and show that their product matches the observations. This has not been done, nor would it likely work owing to nonlinearities.

Response: Thank you for pointing this out. The word “reproduce” is incorrectly used here. The authors want to convey that the GRAPES-CUACE aerosol adjoint model is capable of estimating the sensitivity of concentration to emission sources by **propagating a perturbation in concentration backward** while taking meteorological and chemical processes into consideration.

Therefore, this statement is changed to: This indicates that the GRAPES–CUACE aerosol adjoint model is capable of estimating the sensitivity of concentration to emission sources by propagating a perturbation in concentration **backward in time**, while incorporating meteorological and chemical processes. This presentation is at the end of section 4.2 and is in red.

Claims of efficiency are also implied but not quantified. A single adjoint model integration is often several times (2-10) slower than a normal forward model integration. Thus what is the overall computational savings of their approach here over forward methods, given the size of N and M, quantitatively?

Response: We checked the simulation record and randomly selected five simulation runs for both the



forward and adjoint models. As a result, a single adjoint model integration costs about 2 times computational time that of a normal forward model. For the forward GRAPES-CUACE modeling system, the computational time for integrating 288 steps (1 day) is about 220 min (215 min, 226 min, 226 min, 212 min and 222 min for each selected run). For the GRAPES-CUACE adjoint simulation, the computational time for integrating 288 steps backward is approximately 456 min (448 min, 464 min, 476 min, 443 min and 448 min for each selected run). Besides the high efficiency in computational time of the adjoint model illustrated above, the forward emission sources sensitivity analysis requires repeated adjustment of emissions intensity, which also requires tedious work.

However, adjoint method saves computational time at the expense of large computer storage for state data saving. Despite of it, the adjoint method is still a powerful tool in detecting sensitive emission sources of pollution episodes.

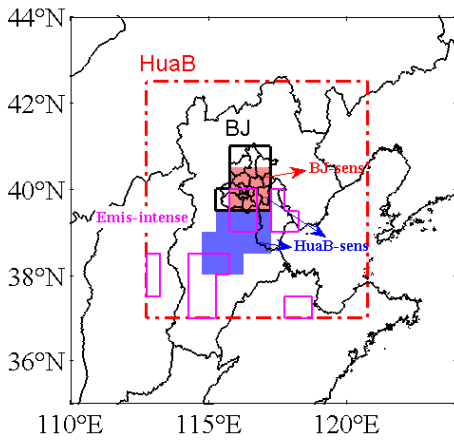
Example of the overall computational savings for the adjoint method over the forward sensitivity calculation: When calculating the changes of a scalar function (concentration) to N source emissions scenarios, N+1 times of forward integration is needed. If using the adjoint method, one forward integration (for state data saving) and one adjoint integration can achieve the sensitivities of the scalar function to the N emission sources at every integration step, much more sensitive information than the forward sensitivity analysis can achieve. Here the forward method costs  $(N+1)*t/2*2t=(N+1)/4$  times computational time of that of the forward sensitivity estimation.

- Fig 6(e) and (f) are good to know, but they are somewhat of a waste of an adjoint model. If the only interest was in the separation between “surrounding” vs “local” emissions of all PM<sub>2.5</sub> precursor emissions, this could have been achieved with only 3 forward model integrations (adjoint not needed). So the authors haven’t really brought out the strength of their results to provide insight into spatial attributions beyond these two regions. Pie chart showing the influence by province, species, and sector would be much more interesting, and would start to approach a level of detail unobtainable without use of an adjoint model.

Response: Thank you very much for your valuable suggestion. We then divided emission sources influence on the average hourly PM<sub>2.5</sub> peaks over Beijing municipality into local Beijing and provinces around Beijing (Hebei province, Tianjin city, Shanxi province and Shandong province). We analyzed the hourly instantaneous sensitivity coefficients of emission sources from each province, their corresponding time-integrated series and the overall contribution proportions of emission sources from each province to the PM<sub>2.5</sub> concentration peaks. Pie charts showing the influence by province are added in Figure 9e and 9f. This part is added in a new section (section 4.4) in the manuscript.

- Fig 8: Defining these ratios based on the area of the regions is not the best idea. It would be better to define the ratios based on the magnitude of the emissions in the different regions, since emissions intensity per unit area is not uniform.

Response: Following the referee’s comments, we further defined an ‘Emis-intense’ region based on the magnitude of the emissions (Fig. 11), and compared its SC/PC (emission sources contribution ratios to peak PM<sub>2.5</sub> concentration peak), S/F(effect) (the ratio of sensitivity coefficients over Emis-intense to the sensitivity coefficients over HuaB, that is the sources contribution effects) and the S/F(efficiency) (the ratios of sensitivity coefficients per unit area over Emis-intense to sensitivity coefficients per unit area over HuaB, that is the sources contribution efficiency). After comparison of the emission sources influence from Emis-intense, HuaB-sens and HuaB, we draw to the conclusion that controlling air pollutant sources from adjoint sensitive emission regions have better effects and higher efficiency than controlling emission sources from emissions intensive regions.



Regions	Number of grid cells	Sensitive area ratios (%)
HuaB-sens	18	10.2
HuaB	176	
BJ-sens	6	60.0
BJ	10	
Emis-intense	18	10.2

Figure 11. Domain definition of Huabei (HuaB, in red dot-dashed frame), Beijing (BJ, in black solid frame), sensitive Beijing (BJ-sens, red shaded), sensitive Huabei (HuaB-sens, red shaded and blue shaded) and emission intensive (Emis-intense, in pink solid frame) regions.

Statistical ratios are added in Table 2 and Table 3 in red. Corresponding analysis are added in section 4.5 in red.

In addition, there are reasons why regions are defined based on the adjoint results: to assess the adjoint sensitive source zone on decreasing  $PM_{2.5}$  concentration over Beijing and to compare the adjoint results with the Models-3/CMAQ assessments. Therefore, through all comparisons in section 4.5, we reach the conclusion that narrowing emission sources reduction scope to sensitive source zones, rather than emission intensive regions, prior to unfavorable meteorological conditions can effectively decrease  $PM_{2.5}$  concentration and improve the efficiency of  $PM_{2.5}$  reduction measures.

- 10.25-28: Table 1 and the argument based on area isn't a great method, as discussed above. And I'm sorry but Table 2 and surrounding discussion just does not make much sense, and requires further clear explanation of what is being presented. What is the importance of the ratio SC/PC? This needs to be explained. What are the percent values percentages of? Do these sum to 100% in some manner? Lastly, comparison to results of Zhai et al. (2016) appears to be entirely qualitative, and no clear summary of how the two compare quantitatively is provided.

Response: SC/PC is the ratios of the time cumulative sensitivity coefficients to peak  $PM_{2.5}$  concentration, and reflects the reduction ratios of peak  $PM_{2.5}$  concentration due to absence in emissions over different regions and during different periods, that is the emission sources contribution ratios to peak  $PM_{2.5}$  concentration. They do not sum to 100% as they are the primary particle sources of  $PM_{2.5}$ . Further clear explanations including the significance of SC/PC, S/F(effect) and S/F(efficiency) are added in section 4.5 in red. Comparisons with results of Zhai et al. (2016) are quantitatively compared by citing quantitative values from the Models-3/CMAQ assessments in the analysis of section 4.5 as well as in Table 2 and Table 3.

### 3. Minor comments

- 2.2: The first sentence is a bit vague, and should be clarified. Adjoint models are efficient for some types of sensitivity calculations, but not all. They are also efficient in terms of wall-time, but not necessarily in terms of memory or i/o.

Response: The adjoint model's efficiency is reflected by its short computational time costs in calculating the sensitivity of a scalar factor with respect to a large number of (input) parameters.



The first and second sentences are revised as:

The atmospheric chemistry adjoint model, developed on the basis of an atmospheric chemistry model according to the adjoint theory, can efficiently calculate sensitivities of a few variables or metrics with respect to a large number of (input) parameters (Sandu et al., 2005; Hakami et al., 2006).

• 2.14-19: This brief overview of “current” applications of adjoint modeling in atmospheric chemistry isn’t a great fit for this paper, as it doesn’t cover the first works in this area, historically, nor is it limited to only the latest works. Also, in attempting to cover all applications of adjoint model, the authors touch upon several areas (O<sub>3</sub>, CO, etc.) that aren’t directly related to the topic of PM<sub>2.5</sub>. I suggest the authors instead consider a more detailed overview of previous works, but one that is more narrowly limited in terms of scope, possibly to just sensitivity studies of PM<sub>2.5</sub>.

Response: Thank you for your suggestion. We revised this paragraph by previous research on the sensitivity studies of PM<sub>2.5</sub>. Detailed responses including changes in the manuscript are presented in the second major comment.

• 3.2: There is a second paper by the same group using adjoint modeling to investigate sources of PM<sub>2.5</sub> in Beijing during the APEC period.

Response: There is a paper using the adjoint of GEOS-Chem to investigate sources of PM<sub>2.5</sub> in Beijing during the APEC period:

Zhang, L., J. Shao, X. Lu, Y. Zhao, Y. Hu, D. K. Henze, H. Liao, S. Gong and Q. Zhang (2016). "Sources and Processes Affecting Fine Particulate Matter Pollution over North China: An Adjoint Analysis of the Beijing APEC Period." *Environmental Science & Technology* 50(16): 8731-8740.

• 3.9: Could the authors clarify what is meant by “guidance on the enactment of dynamic environmental control policy”? What type of policy are they referring to (municipal? national? international?), and what is dynamic about such policy?

Response: ‘Dynamic’ is changed to ‘flexible’.

• 4.13: Technically a first-order finite difference calculation would require N+1 forward model integrations.

Response: Thank you for pointing out this inexact presentation. We changed N to N+1 and added ‘(one base simulation included)’ at the end of the sentence.

• 4.18: The theoretical equivalence of these approaches predates the work of Liu by many decades; I suggest the authors find a more fundamental reference. Also, it is typical to only cite PhD thesis (as opposed to peer reviewed literature) when absolutely necessary, which is not the case here.

Response: We replaced this reference by:

Marchuk, G., *Mathematical Models in Environmental Problems*, Elsevier Science Publication Co., Washington, 1986.

• 4.26: Adjoint sensitivities would only provide “exact” contributions for linear systems. However, PM<sub>2.5</sub> is formed nonlinearly, which needs to be addressed, or the interpretation and use of the adjoint sensitivities needs to be reconsidered.

Response: Thanks for pointing out. This presentation is changed to:

Therefore, we define the sensitivity coefficients in this study as:  $(\partial J / \partial S_n) \cdot S_n$ , which shares the same unit with the objective function, and can reflect the absolute changes in the objective function due to

perturbations in emission sources, thus making comparisons among emissions more convenient.

- 5.14: “Unequilibrated” is not the correct word here. Nonlinear?

Response: Here we want to refer to state variables whose values change with the integration of the forward model. When integrating the adjoint model backward, these saved values are input at each check point to ensure that the forward and the backward models are in the same chemical state. The word ‘unequilibrated’ is used by Henze et al. (2007). Sandu et al. (2005) describe it as ‘the state  $c(x, t)$  saved for all  $t$ ’. To make it clear, we change this part in the manuscript as below, with changes in red:

Figure S3 shows the operational processes in this study. **In order to ensure that the forward and the backward models are in the same chemical state**, the forward GRAPES-CUACE model should be **first** integrated to save the unequilibrated variables **(or called the state concentrations)** in checkpoint files at the beginning of each external time step **(Sandu et al., 2005; Henze et al., 2007)**. **These saved variables were then input** at each check point during the backward adjoint integration. To handle intermediate variables, this study adopted recalculation and stack storage (PUSH & POP) schemes.

- Section 3.2: In addition to the physical processes treated in this aerosol model, please also briefly review what chemistry is included, both in the aerosol and gas-phase, and how the thermodynamic partitioning of species across phases is modeled.

Response: The gas chemistry is based on the second generation of Regional Acid Deposition Model (RADM II) mechanism with 63 gaseous species through 21 photo-chemical reactions and 121 gas phase reactions applicable under a wide variety of environmental conditions especially for smog (Stockwell et al., 1990). Aerosol processes is coherently integrated with the gaseous chemistry in CUACE (Zhou et al., 2012). Since the nitrates and ammonium formed through the gaseous oxidation are unstable and prone to further decomposition back to their precursors, CUACE adopts ISSOROPIA to calculate the thermodynamic equilibrium between them and their gas precursors (Zhou et al., 2012). Relevant model descriptions are added in section 3.2 (underlined in the manuscript).

- Section 3.3: Previous studies have shown that there are influences of emissions on  $PM_{2.5}$  in your receptor cite from beyond the model domain considered here. Thus please explain how the influence from boundary conditions is tracked in the adjoint modeling.

Response: Both the forward and the adjoint model domain covered northeastern China, as shown in Fig. 4 (left). This domain is big enough to take pollutant regional transport into consideration. To better address this problem, we enlarged the cover area in the sensitivity coefficients distribution diagrams in Fig. 7 and Fig. 10. Moreover, we modified the color bars in Fig. 7 and Fig. 10, with values less than 1 amplified in the range of the color bars. Therefore, it is quite clear to see that the value of sensitivity coefficients decreased 2-3 orders of magnitudes to the edge of Fig. 7 and Fig. 10.

Meanwhile, we also enlarged the area when extracting emission sources sensitivity coefficients for the surrounding regions of BJ in section 4.3. Therefore, overall sources contribution ratios from surrounding provinces (add overall contribution ratios from each surrounding province in the pie chart in Fig. 9) are slightly increased compared with the last version of the manuscript.

We hope these changes in the sensitivity coefficients distribution diagrams can help to answer this comments.

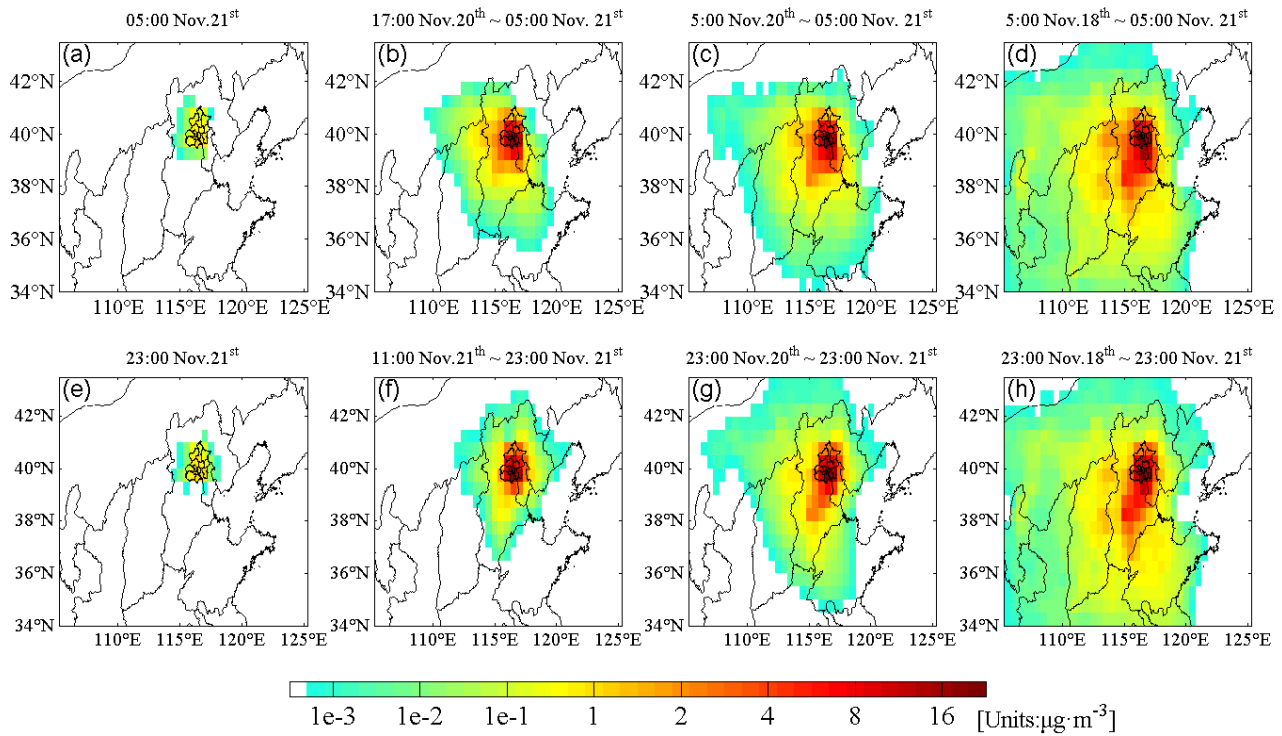


**Figure 7. Time-integrated sensitivity coefficients of surface Beijing PM<sub>2.5</sub> concentration peaks to primary emission sources. (a–d): 1-h, 12-h, 24-h and 72-h integrated sensitivity coefficients for the 5:00 LT on 21 Nov. PM<sub>2.5</sub> concentration peak; (e–h): 1-h, 12-h, 24-h and 72-h integrated sensitivity coefficients for the 23:00 LT on 21 Nov. PM<sub>2.5</sub> concentration peak.**

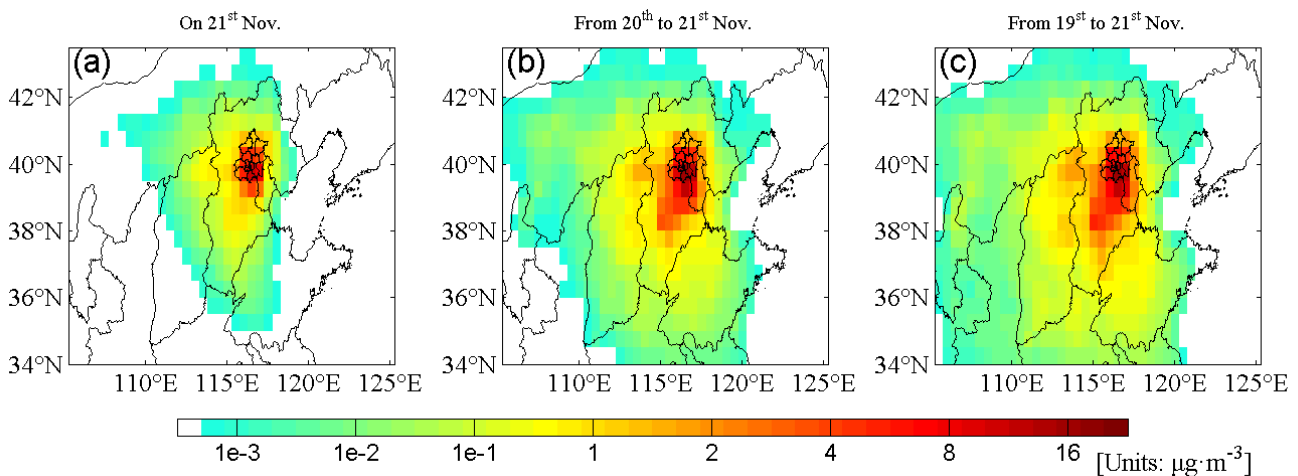


**Figure 10. 24-h (a), 48-h (b) and 72-h (c) integrated sensitivity coefficients of surface PM<sub>2.5</sub> concentrations to primary emission sources in Beijing on 21 Nov. 2012.**

• 7.12: This is a more correct interpretation of adjoint sensitivity results which should be considered in the earlier descriptions.

Response: Thank you. Earlier relevant descriptions are revised to **emphasize** that the adjoint sensitivity reveals the changes in concentration due to small perturbations in emissions sources, in other words, the adjoint model estimates the incremental influence of specific sources on air quality attainment. Corresponding revisions are **green shaded**.

• Fig 5: It appears the emissions continue to spread by 72 hours of back integration. How then did the authors decide to stop the adjoint integration at 72 hrs? In other words, why did they not integrate

backwards further in time? The lifetime of aerosols can be much longer than 3 days, so integration of back to a week to 10 days may be necessary to capture all non-local influences.

Response: From the hourly instantaneous sensitivity coefficients variation in Fig. 8a and 8b and Fig. 9a and 9b, sensitivity coefficients decrease to negligible values (close to zero) after 72 hrs of adjoint integration. Meanwhile, from the time-integrated sensitivity coefficients in Fig. 8c and 8d and Fig. 9c and 9d, time-integrated sensitivity coefficients prone to constant values after 72-hr accumulation.

- Section 4.1: Please clearly define what is meant by “local” in this context. Is it just the single grid cell that contains the Beijing receptor cite?

Response: “Local” refers to the objective region that covers the whole Beijing municipality (both rural and urban Beijing). Definition is added as: local Beijing (the target region that covers the entire Beijing municipality).

- 9.24-26: The non-local contributions do get small after 72 hrs, but as shown in Fig 6(d), the cumulative sensitivities have yet to asymptote to a constant value, which would indicate that sensitivities from early than 72 hrs may still play some role, although small. Also, sensitivities may have transferred to the boundary conditions, as mentioned previously.

Response: As analyzed in section 4.3 and section 4.4, the 23:00 PM<sub>2.5</sub> peak was accumulated on the basis of the 05:00 PM<sub>2.5</sub> peak, and the maximal points on Fig 8b are actually due to the same sources for the maximal points on Fig. 8a. Therefore, the cumulative sensitivities in Fig. 6d (now changed to Fig. 8d) is expected to stop increasing soon afterwards.

#### 4. Corrections

I started making grammatical corrections to the abstract, but stopped after only a few lines, as the entire manuscript needs substantial editing.

- 1.17: in detecting ! to detect
- 1.20: south to ! south of
- 1.21: at the south to ! to the south of

Response: Thank you very much for your revisions.

The above three errors are corrected. Besides, the whole manuscript is edited by the Enago (<http://www.enago.com>) English editing services and verified by the authors. The authors will also order the English copy-editing services from Copernicus.

#### Other Changes in the manuscript:

The title was changed to ‘Detection of critical PM<sub>2.5</sub> emission sources and their contributions to a heavy haze episode in Beijing, China, using an adjoint model’.

Section 3.4 ‘Simulated haze episode’ and section 3.5 ‘Objective function’ are moved to section 4.1 ‘Simulated haze episode and objective function’. Former section 4.1, section 4.2 and section 4.3 are placed to section 4.2, section 4.3 and section 4.5, respectively.

Added analysis of Section 4.4 ‘Emission sources contributions from different provinces around Beijing to peak PM<sub>2.5</sub> concentrations’ and comparisons of emission sources contribution from emission intensive regions and adjoint sensitivity regions are added in section 4.5, the abstract and the conclusion.

## Added References:

Cao G L, Zhang X Y, Gong S L, et al. Emission inventories of primary particles and pollutant gases for China. Chinese Sci Bull, 2011, 56, doi:10.1007/s11434-011-4373-7.

Hakami, A., D. K. Henze, J. H. Seinfeld, K. Singh, A. Sandu, S. Kim, D. Byun and Q. Li (2007). "The adjoint of CMAQ." Environmental science & technology 41(22): 7807-7817.

Sandu, A., D. N. Daescu, G. R. Carmichael and T. Chai (2005). "Adjoint sensitivity analysis of regional air quality models." Journal of Computational Physics 204(1): 222-252.

Stockwell, W. R., Middleton, P., Change, J. S. and Tang, X. 1990. The second generation regional acid deposition model chemical mechanism for regional air quality modeling. J. Geophys. Res. 95, 16343\_16376.

Zhai, S., X. An, Z. Liu, Z. Sun and Q. Hou (2016). "Model assessment of atmospheric pollution control schemes for critical emission regions." Atmospheric Environment 124, Part B: 367-377.

Zhou, C., S. Gong, X. Zhang, H. Liu, M. Xue, G. Cao, X. An, H. Che, Y. Zhang and T. Niu (2012). "Towards the improvements of simulating the chemical and optical properties of Chinese aerosols using an online coupled model – CUACE/Aero." Tellus B 64(0).

## To Short Comment #1

Dear G. Tang,

Thank you very much for your comments. Responses to the comments are listed below in blue:

As for the regional and local contributions for the Beijing haze pollution, we also launched some observation studies, but were not verified by model simulations [G. Tang et al., 2015; Zhu et al., 2016]. After I read this paper, I was so glad that the simulated results were consistent with our findings. However, there were some tiny questions that I want to discuss with the authors:

a. The authors investigated the haze pollution in Beijing based on the two peaks of PM<sub>2.5</sub> concentrations, and the PM<sub>2.5</sub> concentrations were peaked on 05:00 BT and 23:00 BT Nov. 21<sup>st</sup> 2012 respectively. However, these two moments are probably the high pollutant concentration periods originally due to some local emissions (such as the diesel cars). Does it necessary to divide the period so detail? I suppose if it was better to divide the haze episode into two stages, the first stage (from Nov. 19 to 20 2012) may be defined as the early polluted period and the second stage (included the two peaks) may be defined as the heavy polluted period. And then to quantify the regional transport and local contributions.

Response: The high PM<sub>2.5</sub> pollution on Nov. 21<sup>st</sup> 2012 over Beijing is the result of both local and surrounding pollution sources, illustrated in section 4.5 when average PM<sub>2.5</sub> concentration on Nov. 21<sup>st</sup> 2012 over Beijing is set as the objective function and that the relatively more sensitive regions spread over Beijing and surrounding Hebei, Shanxi and Shandong provinces (Fig. 10). **Under the high pollution background on Nov. 21<sup>st</sup> 2012, two hourly PM<sub>2.5</sub> peaks occur.** These two peaks are resulted mainly from the diurnal variation of (planetary boundary layer) PBL with the development of vertical mixing after sunrise for diluting pollutants (added in section 4.1). Meanwhile, from Fig. 7b and 7f, we can see that the 12-hour cumulated sensitivity coefficients mainly concentrated over Beijing, especially for Fig. 7f, reflecting that local source impacting on the pollution peaks dominate 12 hours ahead of the peaks. However, analyzing Figs. 7c, 7d, 7g and 7h, we can see that

surrounding sources emitted 2-3 days ahead have obvious impacts on these two peaks. Besides, analyzing the time-cumulated sensitivity coefficients series (Fig. 8c and 8d) along reversed time sequence, we can see that for both PM<sub>2.5</sub> concentration peaks, the dominant emission source areas transform from the local to the surroundings. **To sum up, these two peaks were due to local impacts at the same day (Nov. 21<sup>st</sup>), but are influenced by local and surrounding sources during the whole pollutants accumulation and polluted episode (18<sup>th</sup>-21<sup>st</sup> Nov. 2012).**

Thank you for your suggestion. We expect it will be an interesting and worthy job to divide the haze episode into two stages as you describe, and we will try to conduct such a simulation in our later work. Here we want to illustrate the applicability of the GRAPES-CUACE aerosol adjoint model in tracking influential PM<sub>2.5</sub> emission source regions and time periods in detail. Especially, to divide the period in detail, the adjoint results clearly illustrate the difference of these two peaks influential sources spatially and temporally, as the first peak is the result of local and surrounding sources accumulation 2-3 days ahead of it, and the second peak is accumulated on the basis of the first peak with dominant influence from local emissions on Nov. 21<sup>st</sup>.

b. Does the obvious periodic fluctuation of hourly sensitivity coefficient of surrounding emissions has some relationship with the mountain-valley winds [Guiqian Tang et al., 2016]?

Response: Yes, the mountain-valley winds have impacts on the periodic fluctuation of hourly sensitivity coefficient of surrounding emissions. When there is no strong weather system, obvious mountain and valley winds appear in the plain area of Beijing-Tianjin-Hebei, and a convergence line shows at the surface layer. During the daytime, valley winds strengthened while mountain winds weakened. During the nighttime, however, mountain winds strengthened while valley winds weakened. Therefore, the convergence line vibrates periodically in the north-south direction, and pollutants accumulated nearby and to the south of the convergence line.

Tang, G., et al. (2016), Mixing layer height and its implications for air pollution over Beijing, China, *Atmospheric Chemistry and Physics*, 16(4), 2459-2475, doi:10.5194/acp-16-2459-2016.

Tang, G., X. Zhu, B. Hu, J. Xin, L. Wang, C. Münkel, G. Mao, and Y. Wang (2015), Impact of emission controls on air quality in Beijing during APEC 2014: lidar ceilometer observations, *Atmospheric Chemistry and Physics*, 15(21), 12667-12680, doi:10.5194/acp-15-12667-2015.

Zhu, X., G. Tang, B. Hu, L. Wang, J. Xin, J. Zhang, Z. Liu, C. Münkel, and Y. Wang (2016), Regional pollution and its formation mechanism over North China Plain: A case study with ceilometer observations and model simulations, *Journal of Geophysical Research: Atmospheres*, 2016JD025730, doi:10.1002/2016JD025730.

#### **Added Reference:**

Tang, G., et al. (2016), Mixing layer height and its implications for air pollution over Beijing, China, *Atmospheric Chemistry and Physics*, 16(4), 2459-2475, doi:10.5194/acp-16-2459-2016.



# Detection of critical PM<sub>2.5</sub> emission sources and their contributions to a heavy haze episode in Beijing, China, using an adjoint model

Shixian Zhai<sup>1</sup>, Xingqin An<sup>2</sup>, Tianliang Zhao<sup>1</sup>, Zhaobin Sun<sup>3,4</sup>, Qing Hou<sup>2</sup>, Chao Wang<sup>2</sup>

<sup>1</sup>Key Laboratory for Aerosol-Cloud-Precipitation of China Meteorological Administration, Collaborative Innovation Center on Forecast and Evaluation of Meteorological Disasters, School of Atmospheric Physics, Nanjing University of Information Science & Technology, Nanjing 210044, China

<sup>2</sup>State Key Laboratory of Severe Weather, Key Laboratory of Atmospheric Chemistry of CMA, Chinese Academy of Meteorological Sciences, Beijing 100081, China

<sup>3</sup>Institute of Urban Meteorology, China Meteorological Administration, Beijing 100089, China

<sup>4</sup>Environmental Meteorology Forecast Center of Beijing-Tianjin-Hebei, China Meteorological Administration, Beijing, 100089, China

*Correspondence to:* Xingqin An (anxq@camsma.cn) and Tianliang Zhao (tlzhao@nuist.edu.cn)

**Abstract.** Air pollutant sources and regional transport are important issues in air quality control. The Global–Regional Assimilation and Prediction System coupled with CMA Unified Atmospheric Chemistry Environment (GRAPES–CUACE) aerosol adjoint model was applied to detect the sensitive emission sources of a haze episode in Beijing during 19–21 November 2012. High PM<sub>2.5</sub> concentration peaks occurred at 05:00 and 23:00 LT (GMT+8) over Beijing municipality on 21 November 2012, which were set as the objective functions for the aerosol adjoint model. The sensitive emission regions of the first PM<sub>2.5</sub> peak were tracked to the west and south of Beijing with 2- to 3-day cumulative transport of air pollutants to Beijing, whereas the sensitive emission regions of the second peak were mainly located to the south of Beijing, where southeasterly moist air transport led to the hygroscopic growth of particles and pollutant convergence in front of the Taihang Mountains in the daytime of 21 November. The temporal variations of the sensitivity coefficients for the two PM<sub>2.5</sub> concentration peaks reveal that the response time of Beijing haze pollution to local emissions is about 1–2 hours, and that to the surrounding emissions is about 7–12 hours. The upstream Hebei province has the largest impacts on the two PM<sub>2.5</sub> concentration peaks, and the contribution of Hebei emissions to the first PM<sub>2.5</sub> concentration peak (43.6%) is greater than to the second PM<sub>2.5</sub> concentration peak (41.5%). The second largest emission contributing province is Beijing (31.2%), followed by Shanxi (9.8%), Tianjin (9.8%) and Shandong (5.7%) for the 05:00 PM<sub>2.5</sub> peak, and Beijing (35.7%) followed by Shanxi (8.1%), Shandong (8.0%) and Tianjin (6.7%) for the 23:00 PM<sub>2.5</sub> peak. The adjoint results were compared with the forward sensitivity simulations of the Models-3/CMAQ system. The two modelling approaches are highly comparable in their assessments of atmospheric pollution control schemes for critical emission regions, but the adjoint method has higher computational efficiency than the forward sensitivity method. This work also reflects that controlling air pollutant sources from adjoint sensitive emission regions has better effects and higher efficiency than controlling emission sources from emission intensive regions.

## 1. Introduction

The application of the adjoint theory to atmospheric chemistry models can enable efficient calculation of sensitivities of a few variables or metrics with respect to a large number of input parameters (Marchuk, 1974; Sandu et al., 2005; Hakami et al., 2007). Classic source-oriented atmospheric chemistry models use inputs of emissions to output the spatial-temporal variation of pollutants. By contrast, receptor-oriented adjoint models take the gradients of the objective function to model variables as inputs, and output the spatial-temporal variations of the sensitivity of the objective function to model parameters (Errico, 1997; Carmichael et al., 2008). Therefore, in concentration source sensitivity analysis problems, the calculation efficiency of the adjoint method is much higher than that of the traditional finite difference method, which requires repeated input perturbations and result comparisons (Wang et al., 2015). Moreover, the finite difference approach changes the state of the modelled atmosphere and inevitably incurs truncation and cancellation errors (Constantin and Barrett, 2014). The adjoint model integrates under certain atmospheric conditions while calculating gradients, and thus can provide exact sensitivities. As a result, if we set the objective function as the pollutant concentration over a region at a point in time (or during a time period), the adjoint sensitivity approach can detect sensitive emission sources in detail by revealing the changes in concentration due to perturbations in emission sources.

Beijing is a rapidly growing economic centre and densely populated metropolis, and its recent PM<sub>2.5</sub> pollution problems have garnered considerable attention (Zhang et al., 2016; Sun et al., 2014; Guo et al., 2010; Wu et al., 2015). PM<sub>2.5</sub> pollution in Beijing is significantly influenced by regional transport of pollutants from its environs, and joint control of air pollutant emission sources has been promoted. Research using approaches like the flux calculation method (An et al., 2007), the back-trajectory model (Zhai et al., 2016), and the observation analysis (Li et al., 2016) have revealed that southerly wind almost always resulted in high PM<sub>2.5</sub> conditions in Beijing. Studies have also pointed out that more than 50% of PM<sub>2.5</sub> pollutants originate in surrounding provinces and cities, including southern Hebei, Tianjin, eastern Shanxi, and Shandong provinces (Jiang et al., 2015; Gao et al., 2016). Studies also show that joint regional air pollution control can be more cost-effective (Wu et al., 2015), and that joint control schemes in sensitive source zones (detected by a back-trajectory model) prior to unfavorable meteorological conditions can help reduce costs and improve efficiency (Zhai et al., 2016). The above studies either provided pollutant pathways through meteorological analysis or analyzed air pollutant concentration sensitivities to a limited group of emission sources. However, if air pollution is spatially and temporally traced back to its emission sources, decision making regarding air pollution can be better addressed.

Differently from back trajectories or statistical factor analysis, the adjoint approach accounts for chemical and physical processes combined with transport, and can efficiently estimate the incremental influence of specific sources on air quality (Henze et al., 2009). Recently, An et al. (2016) developed an adjoint model of GRAPES-CUACE and estimated the

sensitivity of average black carbon (BC) concentrations over Beijing at the highest concentration time with respect to BC amounts emitted over the Beijing–Tianjin–Hebei region and pointed out the effectiveness of controlling the most influential regions during critical time intervals detected by the adjoint sensitivity analysis. Zhang et al. (2015) attributed sources of Beijing  $PM_{2.5}$  using the adjoint GEOS-Chem model and summarized that residential (49.8%) and industrial sources (26.5%) make the largest contributions, and that 45%–53%  $PM_{2.5}$  pollutants in Beijing and Tianjin are from local sources, whereas Hebei province sources contribute about 26%. Both Zhang et al. (2015) and An et al. (2016) showed the high efficiency and accuracy of atmospheric chemistry adjoint model in Beijing air pollutant source apportionment.

In this study, we apply the newly developed GRAPES–CUACE (Global–Regional Assimilation and Prediction System coupled with CMA Unified Atmospheric Chemistry Environment) aerosol adjoint model (An et al., 2016) to track the sensitive emission sources of a high  $PM_{2.5}$  episode in November 2012 Beijing, during which time two  $PM_{2.5}$  concentration peaks occur and are set as the objective functions. By detecting sensitive emission sources of these two hourly  $PM_{2.5}$  peaks, our work advances the understanding of emission source impacts by providing detailed insights into the spatial and temporal variability of emission source contributions from each of the surrounding provinces as well as from local and environs transports. We then set the average  $PM_{2.5}$  concentration on 21 November as the objective function and compared the adjoint results with the Models-3/CMAQ assessments (Zhai et al., 2016). In addition, we also compared emission sources impacts to Beijing  $PM_{2.5}$  peak from adjoint sensitive zones and emission intensive zones. This study explores the capability of the GRAPES–CUACE aerosol adjoint model in simulating the concentration–source relationships in detail and provides guidance for flexible environmental control policy.

## 2. Synoptic analysis of the pollution episode

Atmospheric stability and humidity over the mid-east region of China from 19 to 22 November 2012 were analysed in combination with Meteorological Information Comprehensive Analysis Processing System (MICAPS) results, the sounding stratification and the dew point-pressure curves (temperature-logarithmic pressure diagrams) at Nanjiao Station in Beijing (Figure 1), and the flow field pattern. Meanwhile, the forming processes of two pollution peaks at dawn and at night on 21 November 2012 are also qualitatively analysed. From 19 to 20 November, Beijing was under the influence of a low-pressure system between two high pressures. During the daytime of 19 and 20 November, southerly winds prevail below 925 h Pa and 1000 h Pa, and the relative humidity increased during this time period. During the night-time periods of 19 and 20 November, southerly winds shifted to northeasterly and easterly winds, which brought pollutants together with water vapour to Beijing. Meanwhile, thermal inversions existed below 850hPa during these two days. The above analysis reveals that  $PM_{2.5}$  concentration accumulation was tightly connected with southerly wind during the daytime and the easterly wind at night.

During the daytime on 21 November, the Beijing-Tianjin-Hebei area was at the bottom of a high pressure system, with easterly winds prevailing in the 850hPa layer. The thermal inversion remained, and the relative humidity continued to increase. Mid-south Hebei was influenced by cold air and was controlled by northerly winds, while Beijing was mainly under the influence of an easterly wind that promoted pollutant convergence in front of the Taihang Mountains and carried abundant water vapour which accelerated hygroscopic growth of local particles. It can be concluded that the pollution peak on the night of 21 November is not only the result of pollutant accumulation during the previous 2 days, but also the result of hygroscopic growth of local particles and pollutant convergence caused by the easterly wind during the daytime of 21 November. According to previous research (Chen et al., 2016; Li et al., 2016), this is a typical synoptic episode that gradually generates air pollutants over Beijing until a sudden and significant improvement of air quality results from strong winds. This is also the same episode that is analysed in Zhai et al. (2016), thus facilitating further comparisons.

### 3. Methods

#### 3.1. Concepts of adjoint sensitivity analysis

Sensitivity analysis plays an important role in atmospheric environment research. Knowledge of the impacts of emission sources on pollutant concentrations can help enact effective air pollution control strategies. The adjoint model is efficient at calculating the sensitivity of an objective function to any model variable at any time step. Figure S2 contains schematic diagrams of the forward atmospheric chemistry model and adjoint model. The atmospheric chemistry model takes emissions ( $S$ :  $S_1, S_2, \dots, S_n, \dots, S_N$ ) as inputs and outputs pollutant concentrations ( $C$ :  $C_1, C_2, \dots, C_m, \dots, C_M$ ) through forward integration. Any emission source  $S_n$ , might has an influence on the concentration at any receptor site  $C_m$ . A pair of emission source sensitivity tests, using the traditional source-oriented finite difference method, can obtain the contribution from one emission source (or a combined group of emission sources) to pollutants at any receptor site. Therefore, with  $N$  emission sources and  $M$  receptors in total, the pollutant contribution from each of the  $N$  emission sources to each of the  $M$  receptors (an  $N \times M$  matrix) can be obtained through  $N+1$  iterations of forward integration (one base simulation included).

The receptor-oriented adjoint model is complementary to the forward model. The sensitivity map of a scalar function of pollutant concentration (the objective function) to every emission source ( $N \times 1$  matrix) can be obtained through one backward adjoint integration (Sandu, 2005; An et al., 2016; Zhai, 2015), and the above-mentioned  $N \times M$  matrix requires  $M$  iterations of adjoint integration. Theoretically, the resulting  $N \times M$  matrix from the forward and backward methods are the same within a small perturbation (Marchuk, 1986). Therefore, an atmospheric chemistry model is suitable for simulating air pollution processes, whereas an adjoint model is efficient in quantifying receptor-source relationships. A detailed comparison of the computational costs of forward and adjoint sensitivity analyses can be found in the supplement.

The adjoint model can work out the sensitivity of the objective function  $J$  to any emission source  $S_n$ , denoted  $\partial J/\partial S_n$ . If we compare a group of uniformly distributed emission sources, larger  $\partial J/\partial S_n$  values indicate greater influence of emission source  $S_n$  on  $J$ . However, emission intensities are obviously not uniform between urban and rural areas, and seasonal and diurnal changes add even more nonuniformity. In addition, emissions of different species may have different units and may differ in order of magnitude. Under these circumstances, the relative contribution of each emission source cannot be determined only by the gradient  $\partial J/\partial S_n$ . Therefore, we define the sensitivity coefficients in this study as  $(\partial J/\partial S_n) \cdot S_n$ , which shares the same unit with the objective function, and reflects the absolute changes in the objective function due to perturbations in emission sources, thus making contrast among emissions sources more convenient.

### 3.2. Model description

The GRAPES–CUACE is an online coupled atmospheric chemistry modelling system (Wang et al., 2009; Zhou et al., 2012; Jiang et al., 2015) developed by the China Meteorological Administration (CMA). GRAPES-Meso is a regional meteorological model (Xue et al., 2008) within GRAPES–CUACE, and CUACE is an atmospheric chemistry modelling system independent of meteorological and climate models (Gong et al., 2009). The CUACE system adopted the size-segregated multi-component aerosol algorithm CAM (Canadian Aerosol Module) (Gong et al., 2003) as its aerosol module and the second generation of Regional Acid Deposition Model (RADM II) mechanism (Stockwell et al., 1990) as its gaseous chemistry. CAM contains numerous major aerosol processes in the atmosphere: generation, hygroscopic growth, coagulation, nucleation, condensation, dry deposition/sedimentation, below-cloud scavenging, aerosol activation and chemical transformation of sulphur species in clear air and in clouds (Gong et al., 2003), which is coherently integrated with the gaseous chemistry in CUACE. Since the nitrates and ammonium formed through the gaseous oxidation are unstable and prone to further decomposition back to their precursors, CUACE adopts ISSOROPIA to calculate the thermodynamic equilibrium between them and their gas precursors (Zhou et al., 2012). The CUACE system is compatible with various kinds of meteorological models and can be used as a common platform for atmospheric constituent calculation.

The GRAPES–CUACE aerosol adjoint model was developed by applying adjoint theory to the GRAPES–CUACE modelling system. It includes the adjoint of CAM (Canadian Aerosol Module, Gong et al., 2003), the adjoint of the three interface programmes that connect GRAPES-Meso and CUACE, and the adjoint of the aerosol transport processes. Therefore, the GRAPES–CUACE aerosol adjoint model is capable of coupling major aerosol processes in the atmosphere into its simulations of the sensitivities of the objective function to primary aerosol sources. Therefore,  $S_n$  defined in section 3.1 includes BC, OC, sulphate, nitrate and fugitive dust particles.

Figure S3 shows the operational processes used in this study. In order to ensure that the forward and the backward models were in the same chemical state, the forward GRAPES–CUACE model was first integrated to save the unequilibrated variables (the so-called “state concentrations”) in checkpoint files at the beginning of each external time step (Sandu et al., 2005; Henze et al.,

2007). These saved variables were then input at each cheque point during the backward adjoint integration. To handle intermediate variables, this study adopted recalculation and stack storage (PUSH & POP) schemes. Details about the construction, framework and operational flowchart of the GRAPES–CUACE aerosol adjoint model are discussed in An et al. (2016).

### 3.3. Model setup, data and validation

The simulated domain in this study covered northeast China ( $105^{\circ}\text{E}$ – $125^{\circ}\text{E}$ ,  $32.25^{\circ}\text{N}$ – $42.25^{\circ}\text{N}$ ) (Figure 4), which included  $41 \times 23$  simulation grid cells with 31 vertical layers at the resolution of  $0.5^{\circ} \times 0.5^{\circ}$ . The model integrated at a time step of 300s. The National Centers for Environmental Prediction (NCEP) Final Analysis (FNL) dataset was used to define the initial meteorological field and the meteorological boundary conditions. The initial and boundary values for  $\text{O}_3$  and OH were taken from climatic means and zeros for each aerosol species during the first run, then the daily initial values of all chemical species were determined by the 24-h forecast made by the previous day's simulation. To eliminate the discrepancy between the idealized initial concentration field and the real concentration field, the simulation started at 20:00 Beijing LT (GMT+8) on 10 November 2012 and the analysed period ran from 20:00 LT on 17 November 2012 to 20:00 LT on 22 November 2012.

This study used hourly gridded off-line emission source processed by the SMOKE module, which is based on statistical data from government agencies for 2007 for anthropogenic emissions. Anthropogenic emissions include five aerosol species of black carbon (BC), organic carbon (OC), sulphate, nitrate and fugitive dust particles, in addition to 27 gases, such as VOCs,  $\text{NH}_3$ , CO,  $\text{CO}_2$ ,  $\text{SO}_x$  and  $\text{NO}_x$  (Cao et al., 2011). Emission source types include biomass combustion, residences, power generation, industry, transportation, livestock and poultry breeding, fertilizer use, waste disposal, solvent use, and light industrial product manufacture (Cao et al., 2011). Besides, natural sea salt and natural sand/dust emissions are also calculated in the model.

Figure 2 illustrates the gridded distribution of the overall primary particle sources and Fig. 3 shows the hourly variability of the overall particle sources (as well as sulphate as an example) in Beijing. In Fig. 2, four intensive source zones over Beijing and its surrounding provinces: 1) southern Beijing and Tianjin (TJ), 2) southern Hebei (HB), 3) middle Shanxi (SX) and 4) north central Shandong (SD). Meanwhile, there is a secondary intensive source zone over northern SX. In Fig. 3, overall primary particle source emission intensity decreases to its lowest level at 05:00. Thereafter, emission intensity begins to increase and remains high from 11:00 to 19:00, with a little trough at 14:00. The source intensity temporal profile of every particle species is similar, and sulphate is illustrated for example.

Measurements used in this paper were obtained from the observation stations of Chinese Research Academy of Environmental Sciences (CREAS:  $116.39^{\circ}\text{E}$ ,  $40.03^{\circ}\text{N}$ ), the Guanyuan (GY:  $116.34^{\circ}\text{E}$ ,  $39.93^{\circ}\text{N}$ ) and the Dingling (DL:  $116.22^{\circ}\text{E}$ ,  $40.29^{\circ}\text{N}$ ). The CRAES station locates in northwest Chaoyang District at the Chinese Academy of Environmental Sciences, and the GY station locates at Xicheng district. Both the CREAS station and the GY station are representative urban



observation stations in Beijing. The DL station locates in relatively clean Changping district at northern Beijing and provides background values of observed  $PM_{2.5}$  concentrations.

The reliability of the GRAPES-CUACE modelling system is evaluated by comparisons with hourly  $PM_{2.5}$  concentration observations from 20:00 LT 17 November to 20:00 LT 22 November at CREAS, GY and DL observational stations (Figs. 5a-c, Table 1). Figure 5a-c show the observed and simulated hourly  $PM_{2.5}$  concentration curves from 20:00 LT 17 November to 20:00 LT 22 November, and Table 1 lists the statistical metrics. Figure 5a-c reveal that the results of the GRAPES-CUACE modelling system correspond well with the synoptic analysis of the pollution episode. The modelling system reproduces the  $PM_{2.5}$  accumulation processes from 19 to 21 November in Beijing, and captures the two  $PM_{2.5}$  hourly concentration peaks during the dawn and night of 21 November, as well as the trough during 21 November afternoon at CREAS, GY and DL stations, with correlation coefficients ( $R_s$ ) of 0.87, 0.91 and 0.69, respectively (Table 1). However, the model overestimates  $PM_{2.5}$  concentration values over the period with normalized mean biases (NMBs) of 57.2%, 108.1% and 10.7% at CREAS, GY and DL stations, respectively. The over-estimation is also reflected by positive mean bias (MB) and mean fractional bias (MFB) values. MFBs at CREAS, GY and DL stations are 53.6%, 65.2% and 15.6%, respectively, whereas corresponding mean fractional errors (MFEs) are correspondingly 60.1%, 68.3% and 39.6%. MFEs and MFBs are all within the criteria proposed by Boylan and Russel (2006)—that is, model performance criteria have been met when MFE and the MFB are less than or equal to approximately +75% and  $\pm 60\%$ , respectively—except for the MFB at GY, which is a little high. Model overestimation might be attributable to the coarse resolution of the model settings ( $0.5^\circ \times 0.5^\circ$ ) and local environmental interference at the observation site. Prior studies (Zhou et. al., 2012; Wang et al., 2015a; Wang et. al., 2015b; Jiang et. al., 2015) have proven the stable simulation performance of the GRAPES-CUACE modelling system in reproducing air pollution levels and variation trends over northeast China. Above all, the following analysis mainly focussed on the variations and contribution proportions of emission sources over different regions, so these modelling results can be considered reliable.

## 4. Results

### 4.1. Simulated haze episode and objective function

Figure 6 shows the simulated surface  $PM_{2.5}$  concentration and wind field variations from 17:00 LT on 19 November to 11:00 LT on 22 November. It can be seen that the simulation results are consistent with the qualitative weather analysis of this time period. From 19 to 20 November,  $PM_{2.5}$  accumulated in Beijing under the influence of a convergent wind field pattern: a southerly wind field to the south, an easterly wind field to the east and a westerly wind field to the west. From 5:00 LT to 11:00 LT on 21 November,  $PM_{2.5}$  concentrations exceeded  $550\mu g m^{-3}$  over southern Beijing, south-central Hebei and northwest Tianjin. After this peak,  $PM_{2.5}$  concentration over Beijing, south-central Hebei and Tianjin decreased to a trough in the afternoon, before rising again above  $550\mu g m^{-3}$  at 23:00 LT. The decrease of  $PM_{2.5}$  from the morning to the afternoon was

typical for Beijing, and resulted mainly from diurnal variation of the planetary boundary layer, with vertical mixing after sunrise effectively diluting pollutants (Zhao et al., 2009; Liu et al., 2015; Tang et al., 2016). The concentration peak at 23:00 LT was driven by the influence of the easterly winds, which caused pollutant convergence against the Taihang Mountains, and carried abundant water vapour that promoted local hygroscopic growth. Afterwards, during the daytime of 22 November, a notable northwesterly wind dispersed pollutants in Beijing, thus ending this pollution episode.

Beijing municipality (area that cover both rural and urban Beijing) experienced two hourly  $PM_{2.5}$  concentration peaks at 5:00 LT and 23:00 LT on 21 November (Figure 5d), similar to those observed at the three observation stations. These peaks resulted in the high daily average  $PM_{2.5}$  concentration on 21 November, which was analysed in previous research (Zhai et al., 2016). In order to analyse the critical emission sources of the two hourly  $PM_{2.5}$  concentration peaks, we took advantage of the adjoint model in simulating concentration-emission relationships and defined two objective functions as the hourly mean  $PM_{2.5}$  concentration over Beijing at (i) 5:00 LT and (ii) 23:00 LT on 21 November. To demonstrate the reliability and efficiency of the GRAPES–CUACE aerosol adjoint model to provide guidance toward effective and flexible air quality control designs, a third objective function was defined as (iii) average  $PM_{2.5}$  concentration over Beijing on 21 November. Subsequently, comparisons between results from the GRAPES–CUACE aerosol adjoint model and the Models-3/CMAQ assessments (Zhai et al., 2016) were made.

#### 4.2. Spatial distribution of primary $PM_{2.5}$ emission sources sensitivity coefficients

Figure 7 illustrates the distribution of time-integrated sensitivity coefficients to emission sources for the two concentration peaks in the hourly  $PM_{2.5}$  in Beijing. The sensitivity coefficients of the objective function to emission sources connected pollutants with emissions and revealed the incremental impacts of emissions on peak  $PM_{2.5}$  concentrations. The larger the sensitivity coefficient value is, the greater its influence on the objective function J. For example, the largest sensitivity coefficient in Figure 7d was in the cell that includes Daxing district, with a value of  $22.4\mu\text{g m}^{-3}$ . This indicates that emissions emitted in this area had the greatest influence on the peak concentration when integrated over 72 hours. If emissions were reduced within a small range, decrease of  $PM_{2.5}$  concentration should be linear. For example, if emissions from this cell were reduced by N% from 05:00 LT 18 November to 05:00 LT 21 November, the target  $PM_{2.5}$  concentration would decrease by  $N\%*22.4\mu\text{g m}^{-3}$ .

In Figure 7a and 7d and Figure 7e and 7h, with the accumulation along inverse time sequence, the more influential regions (regions with relatively larger sensitivity coefficients) extended from local Beijing (the target region that covers the entire Beijing municipality) to its surrounding provinces. This phenomenon reflects that in this pollution episode,  $PM_{2.5}$  in Beijing was not only the result of local emissions, but also the result of emissions from surrounding regions, including Hebei province, Tianjin and even Shanxi and Shandong provinces. Emissions from the surrounding areas were continuously transported to Beijing 2 to 3 days ahead of the peak pollution day, leading to the observed increase in Beijing's air pollutant concentration.

There are differences in the variations of the more sensitive emission regions of these two  $PM_{2.5}$  concentration peaks. First, comparing the 12-hour cumulative sensitivity coefficients distribution in Figure 7b and 7f, we can see that emissions to the southwest of Beijing already had a clear influence on the 05:00 LT 21 November  $PM_{2.5}$  concentration peak (Figure 7b), however, for the 23:00 LT 21 November  $PM_{2.5}$  concentration peak, influential emission sources still concentrate over Beijing municipality (Figure 7f), with only a small fraction of influential emissions coming from east and south of Beijing. This is due to the southwesterly airstream positioned to the southwest of Beijing from 23:00 LT on 20 November to 05:00 LT on 21 November and the southeasterly water vapour import during the afternoon and night of 21 November, which caused moisture-absorption growth of local particles and brought pollutants from Tianjin.

Second, it can be seen from the distributions of the 24-h (Figure 7c and 7g) and 72-h (Figure 7d and 7h) cumulative sensitivity coefficients that sensitivity coefficients both in and around Beijing had relatively large values, which reflects that both of these  $PM_{2.5}$  concentration peaks are influenced by local and surrounding emissions. However, the most influential emission regions differed between the two  $PM_{2.5}$  concentration peaks. For the first  $PM_{2.5}$  concentration peak, the key 24-h source regions (Figure 7c) are distributed over Beijing and the west and south of Beijing and the key 72-h source regions (Figure 7g) are to the northeast, in Shanxi province. However for the second  $PM_{2.5}$  concentration peak, the key 24-h source regions are mainly located to the south of Beijing, and the key 72-h source regions are to the west of Beijing (Shanxi province) (Figure 7h), and cover a smaller area than that for the first  $PM_{2.5}$  concentration peak (Figure 7d).

The results of these simulations show that the variation of the sensitivity coefficients distribution, the meteorological condition and the pollution evolution processes correspond with each other very well. This indicates that the GRAPES-CUACE aerosol adjoint model is capable of estimating the sensitivity of concentration to emission sources by propagating a perturbation in concentration backward in time with incorporating meteorological and chemical processes.

#### 4.3. Local and surrounding emission sources influence on peak $PM_{2.5}$ concentrations

Figure 8 illustrates the hourly instantaneous sensitivity coefficients to local and surrounding emission sources (Figure 8a and 8b) and their corresponding time-integrated series (Figure 8c and 8d). The magnitudes of the sensitivity coefficients reflect the incremental influence of local and surrounding emissions to the objective  $PM_{2.5}$  peaks. It can be seen that the instantaneous sensitivity coefficients of the  $PM_{2.5}$  concentration peaks to local (red closed squares) and surrounding (red open squares) emissions ascended to their maximal points before showing a decreasing tendency. However, detailed comparisons of the hourly contribution of local and surrounding emissions revealed their significant differences.

Analysing Figure 8a and 8b along a reversed time sequence, the maximum of the local emission sensitivity coefficients (red closed squares) and the  $PM_{2.5}$  concentration peaks (blue closed circles) appeared at almost the same time, with the latter delayed by 1 to 2 hours. This indicates that local emissions released 1 to 2 hours ahead of the  $PM_{2.5}$  peak values have the largest influence on the peak pollution concentrations. After the sensitivity coefficient maximum points, local emission sensitivity

coefficients decrease sharply to minimal values at 14 hours (for the 05:00 PM<sub>2.5</sub> peak) or 19 hours (for the 23:00 PM<sub>2.5</sub> peak) ahead of the pollution peak and then stay low. This revealed that PM<sub>2.5</sub> generated from local emissions was transported away from Beijing after about 14–19 hours.

In contrast, maximal sensitivity coefficients of the surrounding emissions (red open squares) occurred 7–12 hours ahead of the PM<sub>2.5</sub> concentration peaks (Figure 8a and 8b), which indicates a 7- to 12-hour delay for emissions from surrounding areas to arrive to Beijing. As with backward integration, sensitivity coefficients show overall decreasing trends with periodic fluctuations. For the first PM<sub>2.5</sub> concentration peak (05:00 LT 21 November), three maximal contributions from surrounding areas (Figure 8a) appeared at 17:00 LT 20 November (12 hours ahead of the target time), 1:00 LT 20 November (28 hours ahead of the target time) and 4:00 LT 19 November (49 hours ahead of the target time), respectively, along the reversed time sequence. The first time-reversed relative maximal sensitivity coefficient, at 17:00 LT on 20 November is 7.5 μg m<sup>-3</sup>, while the second and the third time-reversed relative maximal sensitivity coefficients at 1:00 LT on 20 November and 4:00 LT on 19 November are 5.2 μg m<sup>-3</sup> and 1.5 μg m<sup>-3</sup> respectively. For the second PM<sub>2.5</sub> concentration peak (23:00 LT on 21 November) (Figure 8b), the relative maximal contributions from surrounding areas (red open squares) appear at 16:00 LT on 21 November (7 hours ahead of the objective time), 20:00 LT on 20 November (27 hours ahead of the objective time), 23:00 LT on 19 November (48 hours ahead of the objective time) and 3:00 LT 19 November (68 hours ahead of the objective time), and their corresponding sensitivity coefficients are 5.3 μg m<sup>-3</sup>, 5.4 μg m<sup>-3</sup>, 2.6 μg m<sup>-3</sup> and 0.9 μg m<sup>-3</sup> respectively. It is worth noting that sensitivity coefficients maximal points for the 23:00 PM<sub>2.5</sub> peak appear at time points around sensitivity coefficients maximal points for the 05:00 PM<sub>2.5</sub> peak. The sensitivity coefficients around the second maximal contribution, approximately from 17:00 LT on 20 November to 0:00 LT on 21 November, remain at a relatively large value (about 4.7 to 5.4 μg m<sup>-3</sup>), even slightly larger than that of the first maximal sensitivity coefficient. This is because the second PM<sub>2.5</sub> concentration peak is cumulated on the basis of the first high PM<sub>2.5</sub> concentration peak, thus emissions from the surrounding areas from the night on 20 November to early in the morning on 21 November also have a large influence on the second PM<sub>2.5</sub> concentration peak, almost slightly rivalling the influence of the later emissions sensitivity peak.

Based on Figure 8, we can also see that for both PM<sub>2.5</sub> concentration peaks, the dominant emission source areas shifted from the local to the surroundings over backward time sequence (Figs. 8c and 8d). For the first PM<sub>2.5</sub> concentration peak (05:00 LT on 21 November) (Figure 8c), the cumulative local emission sensitivity coefficients (red closed squares) were larger than the surrounding emission sensitivity coefficients (red open squares) from 12:00 LT on 20 November to 05:00 LT on 21 November (lasted for 17 hours), which indicates that local emissions dominated during this 17-hour time period. For the second PM<sub>2.5</sub> concentration peak (23:00 LT on 21 November) (Figure 8d), local emissions dominated from 21:00 LT on 20 November to 23:00 LT on 21 November, which lasted for 26 hours, 9 hours longer than that of the first PM<sub>2.5</sub> peak pollution. This phenomenon again indicates the tiny effect of emissions transport processes on 21 November, and that the increase of PM<sub>2.5</sub>

concentration on 21 November is mainly due to local generation. This reinforces the importance of emissions from surrounding regions in accumulating the first  $PM_{2.5}$  concentration peak.

#### 4.4. Emission sources contributions from different provinces around Beijing to peak $PM_{2.5}$ concentrations

We then divided emission sensitivity coefficients into different provinces over Beijing's surroundings to investigate their influence on the  $PM_{2.5}$  peaks over Beijing municipality. Fig. 9 illustrates the hourly instantaneous sensitivity coefficients to emission sources from Beijing municipality (BJ), Hebei province (HB), Tianjin city (TJ), Shanxi province (SX) and Shandong province (SD) (Figs. 9a and 9b), their corresponding time-integrated series (Figs. 9c and 9d) and the overall contribution proportions of emission sources from each province to the  $PM_{2.5}$  concentration peaks (Figs. 9e and 9f). As shown in Fig. 9, emission sources impacts from BJ, HB, TJ, SX and SD on BJ  $PM_{2.5}$  peaks are quite different in both variation trends and magnitudes.

For the 05:00 of 21 November  $PM_{2.5}$  peak, emission sources from HB contribute the most among surrounding provinces, and HB's hourly sensitivity coefficients variation shows consistent periodic fluctuations with that of surrounding emissions. Three maximal points of the HB hourly sensitivity coefficients variation occur at the same time as that of surrounding emission sources. Corresponding sensitivity coefficients are  $5.3\mu g\ m^{-3}$ ,  $3.2\mu g\ m^{-3}$  and  $0.8\mu g\ m^{-3}$ , respectively (Fig. 9a). The largest influential time period of emissions from TJ appeared 13 h ahead of the objective time (at 16:00 20 November), followed by an obvious secondary maximal point that appeared 24 h ahead of the objective time (at 05:00 20 November). Sensitivity coefficients from SX show a small peak (about  $0.7\mu g\ m^{-3}$ ) 9 h ahead of the objective time (at 20:00 20 November), which is caused by a secondary intensive emission zone in northern SX and relatively close to BJ (Fig. 2). As intensive emission sources in SX and SD are far from BJ (Fig. 2), it took 33–36 h for SX and SD emissions to reach BJ.

For the 23:00 November 21  $PM_{2.5}$  peak, it's worth noting that, except for the maximal sensitivity coefficients of HB and TJ at 16:00 21 November (7 h ahead of 23:00 21 November), prior sensitivity coefficient maximal points appeared at the same time as the maximal points of sensitivity coefficients when the 05:00 21 November  $PM_{2.5}$  concentration peak was set as the objective function. For example, for both  $PM_{2.5}$  concentration peaks, sensitivity coefficients of TJ emission sources reached a maximal point at 16:00 20 November, and SX emission source sensitivity coefficients showed two maximal points at 20:00 20 November and 20:00 19 November in turn. The situations at HB and SD are similar, as even when maximal points do not appear at the exact same time, high value periods are consistent for the two objective functions. The above phenomenon again revealed that the 23:00 21 November  $PM_{2.5}$  concentration peak was accumulated on the basis of the 05:00 21 November  $PM_{2.5}$  concentration peak, and that if the 05:00 21 November  $PM_{2.5}$  concentration peak can be effectively reduced, the  $PM_{2.5}$  concentration peak at 23:00 21 November can be reduced accordingly, thus decreasing the overall  $PM_{2.5}$  concentration on 21 November. These results also reflected the adjoint model's advantage in detecting temporal-spatial sensitive emission sources in detail.

Figs. 9c and 9d show that along the backward time sequence, time-integrated sensitivity coefficients of HB continuously rise after time-integrated sensitivity coefficients of other provinces are prone to remain constant. At around 02:00 to 03:00 20 November, the time-cumulated emissions influence from HB exceeded that from local BJ emissions for both  $PM_{2.5}$  peaks, which reflected that emissions from HB play a leading role in pollutant accumulation for the first BJ  $PM_{2.5}$  peak, and that local emissions influence dominates between the two  $PM_{2.5}$  peaks, that is, during the daytime of 21 November.

The hourly sensitivity coefficients in Figs. 9a and 9b show that emission source impacts from Beijing and each surrounding province decrease to negligible values (close to zero) 72 h ahead of the objective time points. Meanwhile, corresponding time-integrated sensitivity coefficients in Figs. 9c and 9d also stop increasing 72 h prior to the objective time points. Therefore, by integrating sensitivity coefficients 72 hours ahead of the two  $PM_{2.5}$  concentration peaks, we can obtain the overall contribution proportions of emission sources from each province to the BJ  $PM_{2.5}$  peaks (Figs. 9e and 9f). Among all provinces, HB has the largest impact on the two  $PM_{2.5}$  concentration peaks, and the contribution of HB emissions to the first  $PM_{2.5}$  concentration peak (43.6%) is greater than to the second  $PM_{2.5}$  concentration peak (41.5%). The second largest emission source contributing province is Beijing (31.2%), followed by SX (9.8%), TJ (9.8%) and SD (5.7%) for the 05:00  $PM_{2.5}$  peak, and Beijing (35.7%) followed by SX (8.1%), SD (8.0%) and TJ (6.7%) for the 23:00  $PM_{2.5}$  peak.

From all the above analysis, we can conclude that joint control of air pollutant sources with Hebei province, Tianjin city, Shandong and Shanxi provinces 2 to 3 days ahead of the first  $PM_{2.5}$  concentration peak can effectively reduce  $PM_{2.5}$  concentration accumulation due to transported pollutants, thus decreasing the concentrations of the BJ  $PM_{2.5}$  peaks.

#### 4.5. Comparisons of the adjoint results with Models-3/CMAQ assessments

Previous research used a back-trajectory model, FLEXPART, to locate sensitive emission regions of Yanqihu, Beijing in November 2012. The study then used the Models-3/CMAQ modelling system to quantify the effects of emission reduction schemes at different ratios, during different time periods and over different regions on  $PM_{2.5}$  concentration reduction on 21 November in Beijing (Zhai et al., 2016). Based on this, we set the average  $PM_{2.5}$  concentration over Beijing municipality on 21 November as the objective function and compared the adjoint results with the Models-3/CMAQ assessments. Figure 10 illustrates the time-integrated sensitivity coefficient distributions when the Beijing average  $PM_{2.5}$  concentration on 21 November was set as the objective function. The magnitudes of the sensitivity coefficients reflect the incremental influence of emissions to the objective  $PM_{2.5}$  concentration. As with previous research (Zhai et al., 2016) that advocated joint control of emissions with surrounding provinces 2 to 3 days ahead of the most polluted day, adjoint time-integrated sensitivity intensified and extended during 48- to 72-h backward time integration.

In order to assess the adjoint sensitive source zone on decreasing  $PM_{2.5}$  concentration over Beijing and to compare the adjoint results with the Models-3/CMAQ assessments, we referred to the research by Zhai et al. (2016) and selected four emission regions: the overall Huabei region (HuaB), the sensitive Huabei region (HuaB-sens), the overall Beijing municipality (BJ) and



the sensitive Beijing region (BJ-sens) (Figure 11). Grid cells with 72-h cumulative sensitivity coefficients larger than  $3\mu\text{g m}^{-3}$  were included in the sensitive emission regions (HuaB-sens and BJ-sens), and grid cells with smaller sensitive values are outside the sensitive emission regions. Therefore, sensitive emission regions have relatively larger impact on the  $\text{PM}_{2.5}$  peak concentrations than regions outside them. Here the HuaB-sens accounts for 10.2% the area of HuaB and the BJ-sens accounts for 60.0% the area of BJ, which makes them analogous to the regions defined by Zhai et al. (2016). In the work by Zhai et al. (2016), HuaB-sens accounts for 17.6% of the area of HuaB and BJ-sens accounts for 54.2% of the area of BJ. In addition, based on emission magnitudes (Fig. 2), we defined regions with emission intensities larger than  $4.1 \times 10^{-7} \text{g} \cdot \text{s}^{-1}$  within HuaB as the “Emis-intensive” regions (Fig. 11). The Emis-intensive region has the same area as that of the HuaB-sens.

Table 2 lists the ratios of the time cumulative sensitivity coefficients to peak  $\text{PM}_{2.5}$  concentration (SC/PC) over the BJ, BJ-sens, HuaB, HuaB-sens, and Emis-intensive regions at 3 different time points: 0 days (d0), 1 day (d1) and 2 days (d2) in advance of the most polluted day. The SC/PC reflects the reduction ratios of peak  $\text{PM}_{2.5}$  concentration due to absence of emissions over different regions and during different periods, that is, emission source contribution ratios to peak  $\text{PM}_{2.5}$  concentration. From Table 2, we can see that the adjoint results are highly consistent with the Models-3/CMAQ system results (Zhai et al., 2016). The 21 November  $\text{PM}_{2.5}$  concentration was an accumulated result from emissions released in the day or two days leading up to the most polluted day, rather than a simple result of emissions on 21 November. For all the BJ, BJ-sens, HuaB and HuaB-sens regions, emissions contribution ratios grew from ‘d0’ to ‘d2’ (‘d0’, ‘d1’ and ‘d2’ are defined in the caption of Table 2), especially from ‘d0’ to ‘d1’. The contribution ratios of emissions from BJ (and BJ-sens) and HuaB (and HuaB-sens) increased by 6.2% (5.8%) and 31.9% (18.9%), respectively, from ‘d0’ to ‘d1’. Thereafter, the contribution ratios again increased by 0.6% (0.5%) and 9.6% (3.6%), respectively, for emissions over BJ (or BJ-sens) and HuaB (or HuaB-sens) from ‘d1’ to ‘d2’. The above phenomenon also indicates that, with the accumulation of time-reversed integration from 48h to 72h prior to 21 November, emission source contributions from HuaB (or HuaB-sens) to peak  $\text{PM}_{2.5}$  concentration increases more obviously, while emission source contributions from BJ (or BJ-sens) hardly increase at all. This can be explained by surrounding emissions being continuously transported to Beijing 2 to 3 days ahead of the most polluted day (Zhai et al., 2016). Similarly to the work in Models-3/CMAQ assessments, Table 3 shows comparisons of sensitive emission, full emission, and Emis-intensive region source contribution effects and efficiencies to peak  $\text{PM}_{2.5}$  concentration. In Table 3, S/F(effect) in the BJ-sens column refers to the ratios of sensitivity coefficients over BJ-sens to sensitivity coefficients over BJ, and S/F(effect) in the HuaB-sens (or the Emis-intensive) column refers to the ratios of sensitivity coefficients over HuaB-sens (or Emis-intensive) to sensitivity coefficients over HuaB. Correspondingly, S/F(efficiency) refers to the ratios of sensitivity coefficients per unit area over BJ-sens (or over HuaB-sens and Emis-intensive) to sensitivity coefficients per unit area over BJ (or over HuaB). Therefore, S/F(effect) and S/F(efficiency) reflect emission source reduction effects and reduction efficiency over sensitive (or emission intensive) regions. The implication of ‘d0’, ‘d1’ and ‘d2’ in Table 3 are the same as they are in

Table 2. As shown in Table 3, the contribution efficiencies (contribution ratios per unit area) of emissions from the HuaB-sens and BJ-sens are significantly higher than those from the corresponding entire HuaB and BJ regions respectively. Although BJ-sens covers only 60% the area of the entire BJ, its contribution to the peak  $PM_{2.5}$  concentration is 86.6%–88.2% of that of the entire BJ. Its source contribution efficiency is 1.4 to 1.5 times that of BJ. Similarly, HuaB-sens covers only 10.2% the area of the entire HuaB, its contribution to the peak  $PM_{2.5}$  concentration is 61.0%–71.9% of that of the entire HuaB, and its source contribution efficiency is 6.0-7.0 times that of the entire HuaB (Table 3). Finally, emissions from HuaB-sens contribute much more than emissions only from BJ-sens, which supports joint control. Analogously, in the Models-3/CMAQ assessments, BJ-sens (or HuaB-sens) covers 54.2% (or 17.6) the area of BJ (or HuaB), and its emissions reduction effect is 99.2%–100% (or 87.2%-93.7%) of that of the entire BJ (or HuaB), and its source contribution efficiency is 1.8 to 1.9 times (or 5.0 to 5.3 times) that of BJ (or HuaB).

We then compared emission source contribution ratios, effect and efficiency from the HuaB-sens and the Emis-intense regions. As shown in Table 2 and Table 3, although the Emis-intense region has the same area as HuaB-sens, its SC/PC, S/F (effect) and S/F (efficiency) are all much smaller. The source contribution ratios to  $PM_{2.5}$  concentration on 21 November (SC/PC) from ‘Emis-intense’ are 9.7%, 17.6% and 18.5% smaller than those from HuaB-sens (Table 2), and the source contribution effect from ‘Emis-intense’ regions (S/F (effect)) are 37.9%, 30.7% and 27.6% smaller than the S/F (effect) of HuaB-sens, indicating that controlling air pollutant sources from adjoint sensitive emission regions has better effects and higher efficiency than controlling emission sources from emission-intensive regions.

The computational loads of the adjoint simulation were much smaller than the comparable assessments made with the Models-3/CMAQ modelling (Zhai et al., 2016). For the adjoint simulation, one forward integration (for un-equilibrated data saving) and one backward adjoint integration can obtain the influence of emissions from any source region, during any time period to  $PM_{2.5}$  peaks. For the Models-3/CMAQ assessments, to compare the effects of emission reductions over two different time periods, at two different ratios and over four different regions, 12 sensitivity tests with a control simulation are required.

## 5. Conclusions

In this research, the GRAPES–CUACE aerosol adjoint model was applied to detect the pivotal emission sources of a November 2012 haze episode, and the hourly peak  $PM_{2.5}$  concentrations at 05:00 LT and 23:00 LT on 21 November 2012 over Beijing were set as the objective functions. Contributions to  $PM_{2.5}$  concentration peaks from local Beijing and its surrounding provinces were compared. The adjoint results correspond well with the real weather analysis for this period, and correctly describe the spatial distribution of the most influential emission sources over time for both  $PM_{2.5}$  concentration peaks. The 05:00  $PM_{2.5}$  concentration peak was mainly influenced by local Beijing emissions, and the emissions from Hebei, Tianjin and Shanxi, due to transmission of pollutants 2 to 3 days ahead of the peak time. The 23:00  $PM_{2.5}$  concentration peak was more

sensitive to local Beijing emissions, and the regions to the south of Beijing, in Hebei province, because of accumulation from the first PM<sub>2.5</sub> concentration peak and local particle hygroscopic growth and pollutants trapped against of the Taihang Mountains on 21 November. The upstream Hebei province has the largest impacts on both PM<sub>2.5</sub> concentration peaks, and the contribution of Hebei emissions to the first PM<sub>2.5</sub> concentration peak (43.6%) is greater than to the second PM<sub>2.5</sub> concentration peak (41.5%). In Beijing, PM<sub>2.5</sub> concentration peaks respond to local emissions in 1 to 2 hours, while surrounding emissions take 7 to 12 hours to influence Beijing's air quality.

We compared the adjoint results with Models-3/CMAQ assessments and found that the adjoint results can provide evidence for all the conclusions supported by the Models-3/CMAQ assessments (Zhai et al., 2016). We then defined the 'Emis-intense' region as an emission-intensive region within Huabei region that has the same area of that of sensitive Huabei region (HuaB-sens) and compared its emission source contributions with those of HuaB-sens and Huabei. Overall, we concluded that narrowing emission sources reduction scope to sensitive source zones (zones detected by an adjoint model or a FLEXPART model), rather than emission intensive regions, 2 to 3 days prior to unfavorable meteorological conditions can effectively decrease PM<sub>2.5</sub> concentration and improve the efficiency of PM<sub>2.5</sub> reduction measures. Meanwhile, the adjoint simulation is far more computationally efficient than the assessments with Models-3/CMAQ modelling. The adjoint method is a powerful tool for simulating the relationship between emissions and concentrations, and it can be utilised to help improve flexible air quality control schemes.

## References:

- An, X. Q., Zhai, S. X., Jin, M., Gong, S. L., and Wang, Y.: Development of an adjoint model of GRAPES–CUACE and its application in tracking influential haze source areas in north China, *Geosci. Model Dev.*, 9, 2153-2165, 2016.
- An, X. Q., Zhu, T., Wang, Z. F., Li, C. Y., and Wang, Y. S.: A modeling analysis of a heavy air pollution episode occurred in Beijing, *Atmos. Chem. Phys.*, 7(12), 3103-3114, 2007.
- Cao, G. L., Zhang, X. Y., Gong, S. L., An, X. Q., Wang, Y. Q.: Emission inventories of primary particles and pollutant gases for China. *Chinese Sci Bull*, 56, doi:10.1007/s11434-011-4373-7, 2011.
- Carmichael, G. R., Sandu, A., Chai, T. F., Daescu, N. D., Constantinescu, E. M., and Tang Y. H.: Predicting air quality: Improvements through advanced methods to integrate models and measurements, *Journal of Computational Physics.*, 227(7): 3540-3571, 2008.
- Constantin, B. V. and Barrett, S. R.: Application of the complex step method to chemistry-transport modeling, *Atmos. Environ.*, 99: 457-465, 2014.
- Chen, Z. Y., Xu, B., Cai, J., and Gao B. B.: Understanding temporal patterns and characteristics of air quality in Beijing: A local and regional perspective, *Atmos. Environ.*, 127: 303-315, 2016.

- Errico, R. M.: What is an adjoint model? *Bulletin of the American Meteorological Society*, 78(11), 2577-2591, 1997.
- Gao, M., Carmichael, G. R., Wang, Y., Saide, P. E., Yu, M., Xin, J., Liu, Z., and Wang, Z.: Modeling study of the 2010 regional haze event in the North China Plain, *Atmos. Chem. Phys.*, 16(3), 1673-1691, 2016.
- Guo, Y. M., Tong, S. L., Li, S. S., Barnett, A. G., Yu, W. W., Zhang, Y. S., and Pan, X. C.: Gaseous air pollution and emergency hospital visits for hypertension in Beijing, China: a time-stratified case-crossover study, *Environmental Health*, 9(1), 57, 2010.
- Hakami, A., Henze, D. K., Seinfeld, J. H., Singh, K., Sandu, A., Kim, S., Byun, D. and Li, Q.: The adjoint of CMAQ. *Environmental science & technology* 41(22): 7807-7817, 2007.
- Henze, D. K., Seinfeld, J. H., and Shindell, D. T.: Inverse modeling and mapping US air quality influences of inorganic PM<sub>2.5</sub> precursor emissions using the adjoint of GEOS-Chem, *Atmos. Chem. and Phys.*, 9(16), 5877-5903, 2009.
- Jiang, C., Wang H., Zhao T. L., Li T., and Che H.: Modeling study of PM<sub>2.5</sub> pollutant transport across cities in China's Jing-Jin-Ji region during a severe haze episode in December 2013, *Atmos. Chem. Phys.*, 15(10), 5803-5814, 2015.
- Li, L. J., Wang, Z. S., Zhang, D. W., Chen, T., Jiang, L., and Li, Y. T.: Analysis of heavy air pollution episodes in Beijing during 2013-2014, *China Environmental Science*, 36(1): 27-35, 2016 (in Chinese).
- Liu, Z., Hu, B., Wang, L., Wu, F., Gao, W., and Wang, Y.: Seasonal and diurnal variation in particulate matter (PM<sub>10</sub> and PM<sub>2.5</sub>) at an urban site of Beijing: analyses from a 9-year study, *Environmental Science and Pollution Research*, 22, 627-642, 2015.
- Marchuk, G.: Numerical solution of the problems of the dynamics of the atmosphere and the ocean (In Russian), *Gidrometeoizdat*, 1974.
- Sandu, A., Daescu, D. N., Carmichael, G. R., and Chai, T.: Adjoint sensitivity analysis of regional air quality models, *Journal of Computational Physics*, 204, 222-252, 2005.
- Sun, Y. L., Jiang, Q., Wang, Z., Fu, P. Q., Li, J., Yang T., and Yin, Y.: Investigation of the sources and evolution processes of severe haze pollution in Beijing in January 2013, *Journal of Geophysical Research: Atmospheres*, 119(7), 4380-4398, 2014.
- Stockwell, W. R., Middleton, P., Change, J. S. and Tang, X.: The second generation regional acid deposition model chemical mechanism for regional air quality modeling. *J. Geophys. Res.* 95, 16343\_16376, 1990.
- Tang, G., Zhang, J., Zhu, X., Song, T., Munkel, C., Hu, B., Schäfer, K., Liu, Z., Zhang, J., Wang, L., Xin, J., Suppan, P. and Wang, Y.: Mixing layer height and its implications for air pollution over Beijing, China. *Atmos. Chem. Phys.* 16(4): 2459-2475, 2016.
- Wang, H., Shi, G. Y., Zhang, X. Y., Gong, S. L., Tan, S. C., Chen, B., Che, H. Z., and Li, T.: Mesoscale modelling study of the interactions between aerosols and PBL meteorology during a haze episode in China Jing-Jin-Ji and its near surrounding region – Part 2: Aerosols' radiative feedback effects, *Atmos. Chem. Phys.*, 15, 3277-3287, 2015a.
- Wang, H., Xue, M., Zhang, X. Y., Liu, H. L., Zhou, C. H., Tan, S. C., Che, H. Z., Chen, B., and Li, T.: Mesoscale modelling

study of the interactions between aerosols and PBL meteorology during a haze episode in Jing-Jin-Ji (China) and its nearby surrounding region – Part 1: Aerosol distributions and meteorological features, *Atmos. Chem. Phys.*, 15, 3257-3275, 2015b.

Wang, L. T., Wei, Z., Wei, W., Fu, J. S., Meng, C. C., and Ma, S.: Source apportionment of PM<sub>2.5</sub> in top polluted cities in Hebei, China using the CMAQ model, *Atmos. Environ.*, 122, 723-736, 2015.

Wu, D., Xu, Y., and Zhang S. Q.: Will joint regional air pollution control be more cost-effective? An empirical study of China's Beijing–Tianjin–Hebei region, *Journal of Environmental Management*, 149, 27-36, 2015.

Xue, J. and Chen, D.: *Scientific Design and Application of Numerical Predicting System GRAPES*, Science Press, Beijing, 2008.

Zhai, S. X., An, X. Q., Liu, Z., Sun, Z. B., and Hou, Q.: Model assessment of atmospheric pollution control schemes for critical emission regions, *Atmos. Environ.*, 124, Part B, 367-377, 2016.

Zhang, H. F., Wang, S. X., Hao, J. M., Wang, X. M., Wang, S. L., Chai, F. H., and Li, M.: Air pollution and control action in Beijing, *Journal of Cleaner Production*, 112, Part 2: 1519-1527, 2016.

Zhang, L., Liu, L. C., Zhao, Y. H., Gong, S. L., Zhang, X. Y., Henze, D. K., Capps, S. L., Fu, T. M., Zhang, Q., and Wang, Y. X.: Source attribution of particulate matter pollution over North China with the adjoint method, *Environmental Research Letters* 10(8): 084011, 2015.

Zhou C. H., Gong S. L., Zhang X. Y., Liu H. L., Xue M., Cao G. L., An X. Q., Che H. Z., Zhang Y. M., and Niu T.: Towards the improvements of simulating the chemical and optical properties of Chinese aerosols using an online coupled model – CUACE/Aero, *Tellus B*, 64(0), 2012.

Table 1 Performance statistics of PM<sub>2.5</sub> concentration.

Simulated Time Period	Stations	Obs. (μg·m <sup>-3</sup> )	Sim. (μg·m <sup>-3</sup> )	R	MB (μg·m <sup>-3</sup> )	NMB (%)	NME (%)	MFB (%)	MFE (%)
20:00 Nov. 17-22, 2012	CREAS	121.5	190.9	0.87	69.4	57.2	185.2	53.6	60.1
	GY	139.0	289.4	0.91	150.4	108.1	183.3	65.2	68.3
	DL	101.4	112.2	0.69	10.8	10.7	85.6	15.6	39.6

Notes: Mean bias:  $MB = \frac{1}{n} \sum_{i=1}^n (Sim_i - Obs_i)$ ;

Normalized mean bias:  $NMB = \frac{\sum_{i=1}^n (Sim_i - Obs_i)}{\sum_{i=1}^n Obs_i} \times 100\%$ ; Normal mean error:  $NME = \frac{1}{n} \sum_{i=1}^n \frac{|Sim_i - Obs_i|}{Obs_i} \times 100\%$ ;

Mean fractional bias:  $MFB = \frac{1}{N} \sum_{i=1}^N \frac{(Sim_i - Obs_i)}{(Obs_i + Sim_i/2)}$ ; Mean fractional error:  $MFE = \frac{1}{N} \sum_{i=1}^N \frac{|Sim_i - Obs_i|}{(Obs_i + Sim_i/2)}$

Table 2 Emission sources contribution to the average PM<sub>2.5</sub> concentration over Beijing on Nov 21<sup>st</sup>.

Factors	Time period	BJ	BJ-sens	HuaB	HuaB-sens	Emis-intense
SC/PC	d0	14.5%	12.5%	25.6%	18.4%	8.7%
	d1	20.7%	18.3%	57.5%	37.3%	19.7%
	d2	21.3%	18.8%	67.1%	40.9%	22.4%

Notes: d0 refers to emissions contribution from 21 November; d1 refers to emissions contribution from 20 to 21 November; d2 refers to emissions contribution from 19 to 21 November

SC/PC='time cumulative Sensitivity Coefficient'/'Peak Concentration';

Table 3 Contrast of sensitive (or emis-intense) and full regions emission sources contribution

GRAPES-CUACE aerosol adjoint model results					Models-3/CMAQ results (Zhai et al., 2016)	
Time period	Factors	BJ-sens	HuaB-sens	Emis-intense	BJ-sens	HuaB-sens
d0	S/F(effect)	86.6%	71.9%	34.0%		
	S/F(efficiency)	1.4	7.0	3.3		
d1	S/F(effect)	88.2%	64.9%	34.2%	99.2%	93.7%
	S/F(efficiency)	1.5	6.3	3.3	1.8	5.3
d2	S/F(effect)	88.2%	61.0%	33.4%	100.8%	87.2%
	S/F(efficiency)	1.5	6.0	3.3	1.9	5.0

Notes: S/F(effect) = 'Sensitivity Coefficient over sensitive source region'/'Sensitivity Coefficient over corresponding full source region';

Contribution Efficiency = 'Sensitivity Coefficient'/'Number of region's simulation grid cells';

S/F(efficiency) = 'Contribution Efficiency of sensitive region'/'Contribution Efficiency of corresponding full source region'.



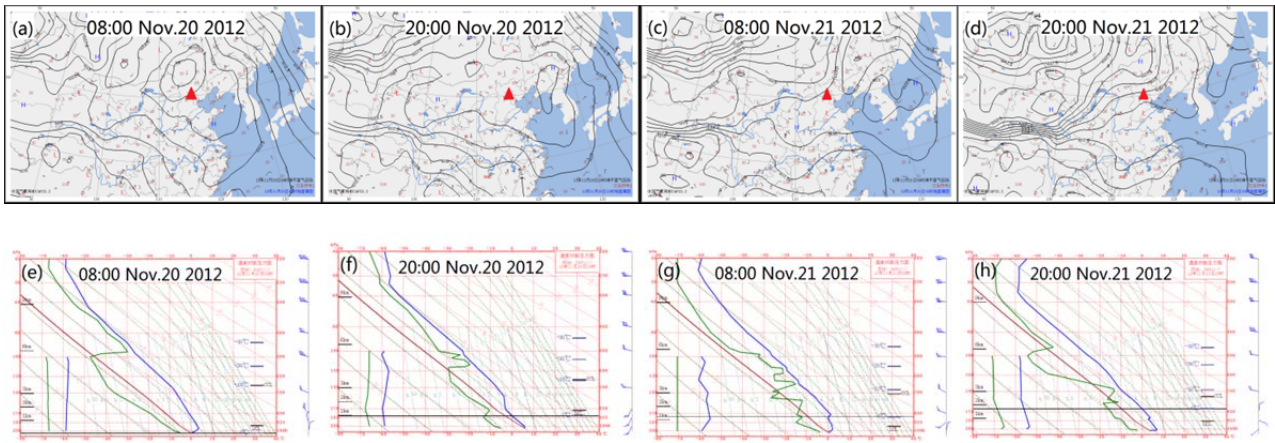


**Figure 1.** (a–d): Sea-level pressure field (black contour lines; Beijing is marked with red triangle); (e–h): temperature-logarithmic pressure diagrams (thick red solid curves **indicate** process; green solid curves **indicate** dew point-pressure; blue solid curves **indicate** stratification) at Nanjiao Station from 08:00 (local time) on 20 November 2012 to 20:00 (local time) on 21 November 2012. Detailed information in Fig. S1.

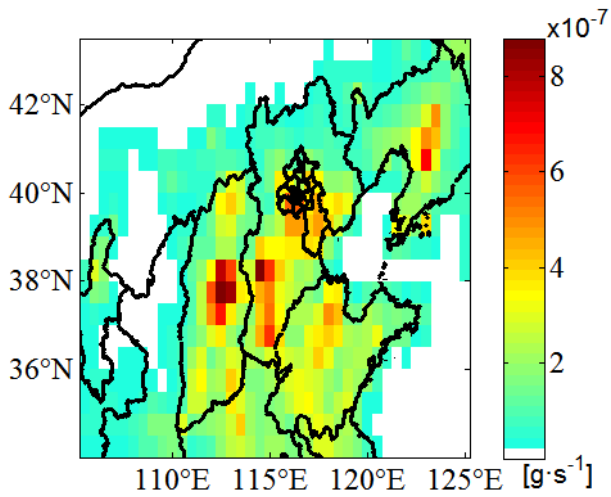


**Figure 2.** Gridded distribution of  $PM_{2.5}$  primary emission sources.

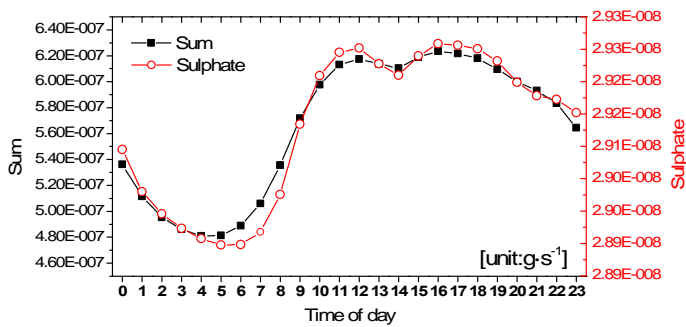


**Figure 3.** Hourly variation of primary  $PM_{2.5}$  emission sources in Beijing.

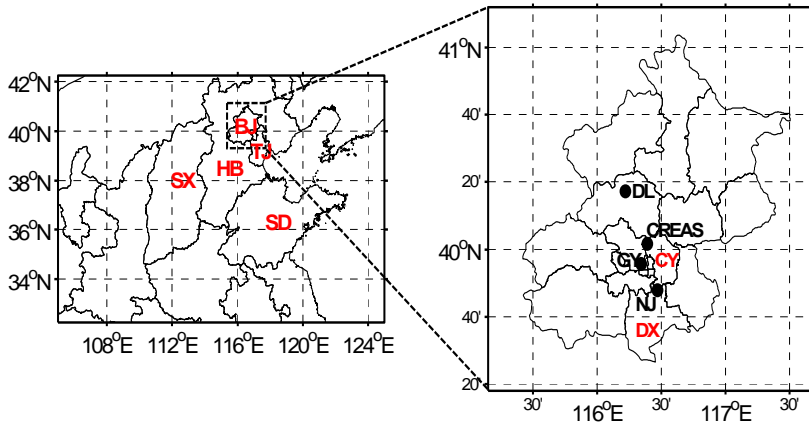


Figure 4. Left: Model domain and location of Beijing municipality (BJ), Tianjin municipality (TJ), Hebei province (HB), Shandong province (SD) and Shanxi province (SX); right: Locations of the Chinese Research Academy of Environmental Sciences (CREAS) station, the Guanyuan (GY) station, the Dingling (DL) station, the Nanjiao (NJ) station, Daxing district (DX) and Chaoyang (CY) district.

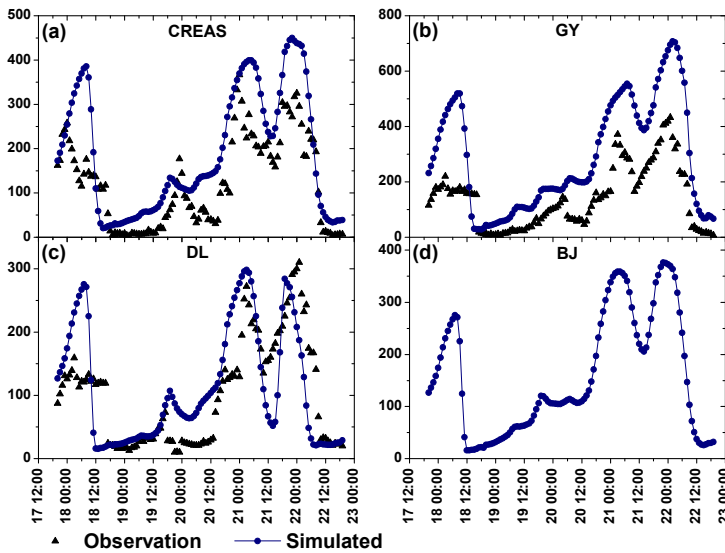


Figure 5. (a)-(c): Comparisons of the observed (black solid triangles) and simulated (blue dot-line) hourly  $PM_{2.5}$  concentrations at CREAS station, GY station and DL station; (d): Hourly variations of average  $PM_{2.5}$  concentration over Beijing municipality.

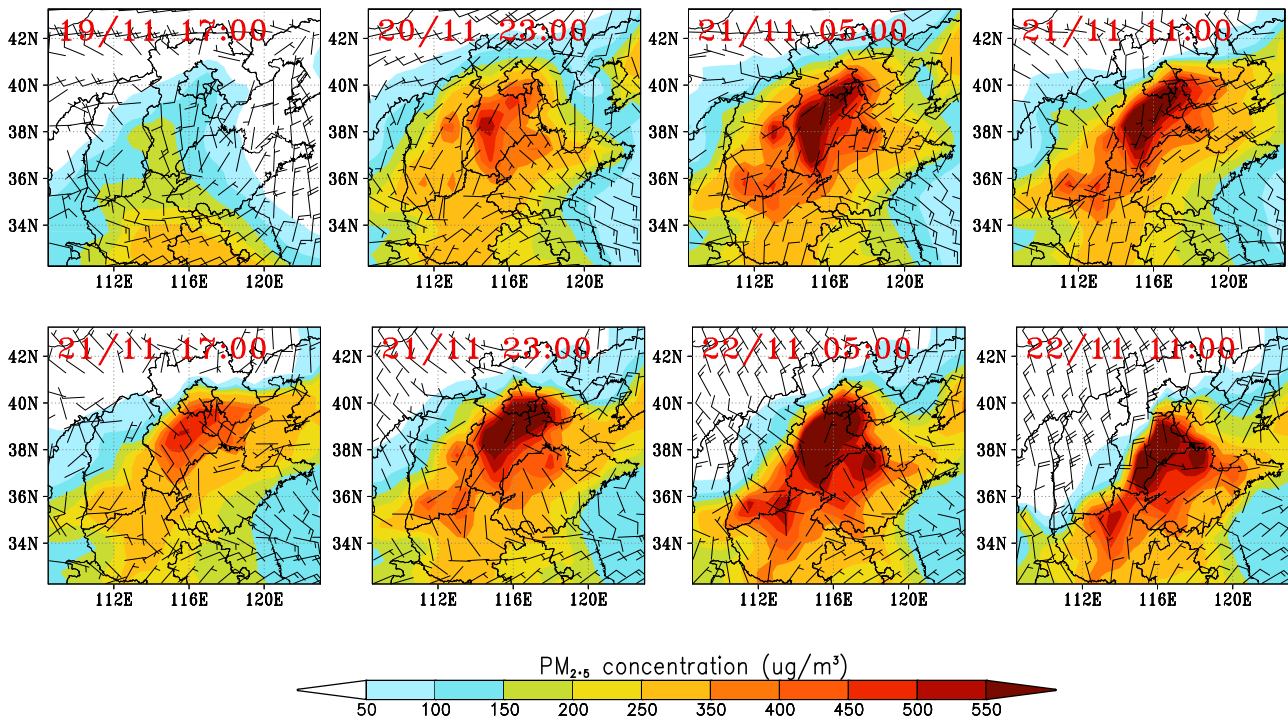


Figure 6. Variations of simulated surface  $PM_{2.5}$  concentration and wind field distributions.

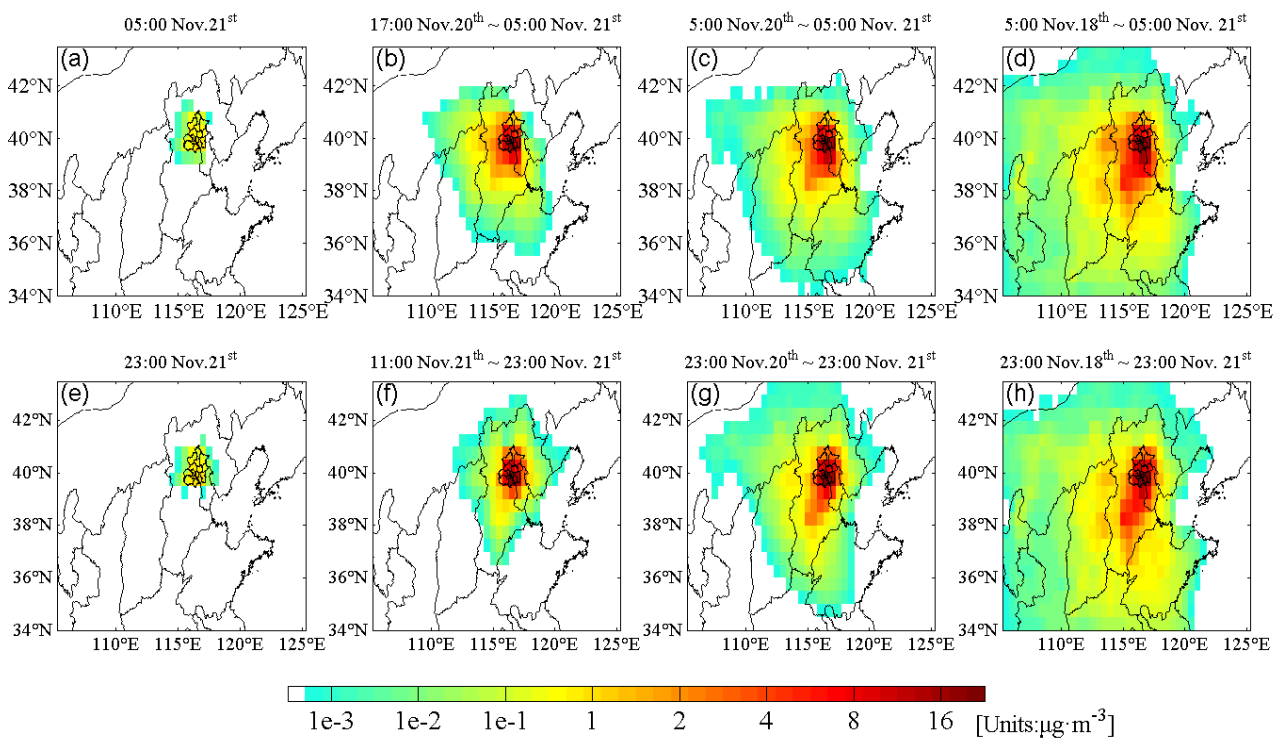


Figure 7. Time-integrated sensitivity coefficients of surface Beijing  $PM_{2.5}$  concentration peaks to primary emission sources. (a–d): 1-h, 12-h, 24-h and 72-h integrated sensitivity coefficients for the 5:00 LT on 21 November  $PM_{2.5}$  concentration peak; (e–h): 1-h, 12-h, 24-h and 72-h integrated sensitivity coefficients for the 23:00 LT on 21 November  $PM_{2.5}$  concentration peak.

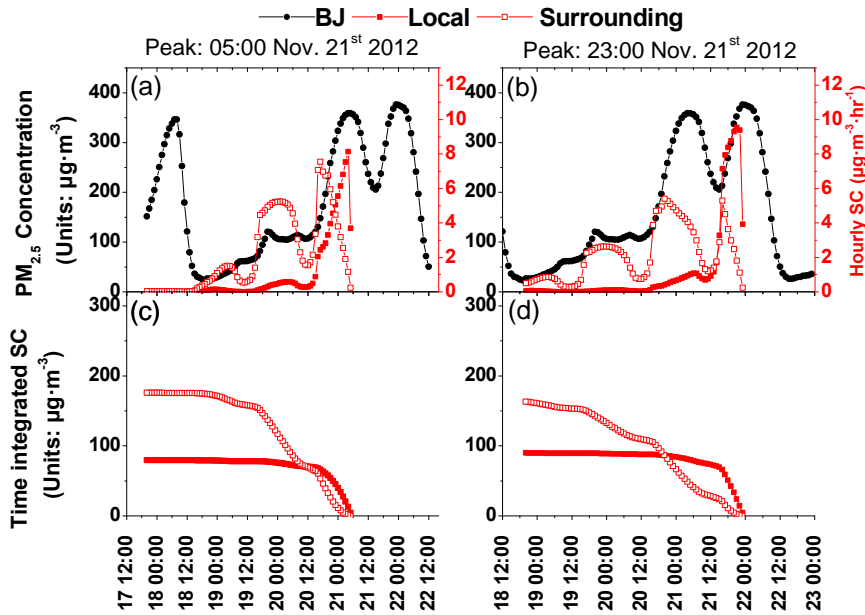
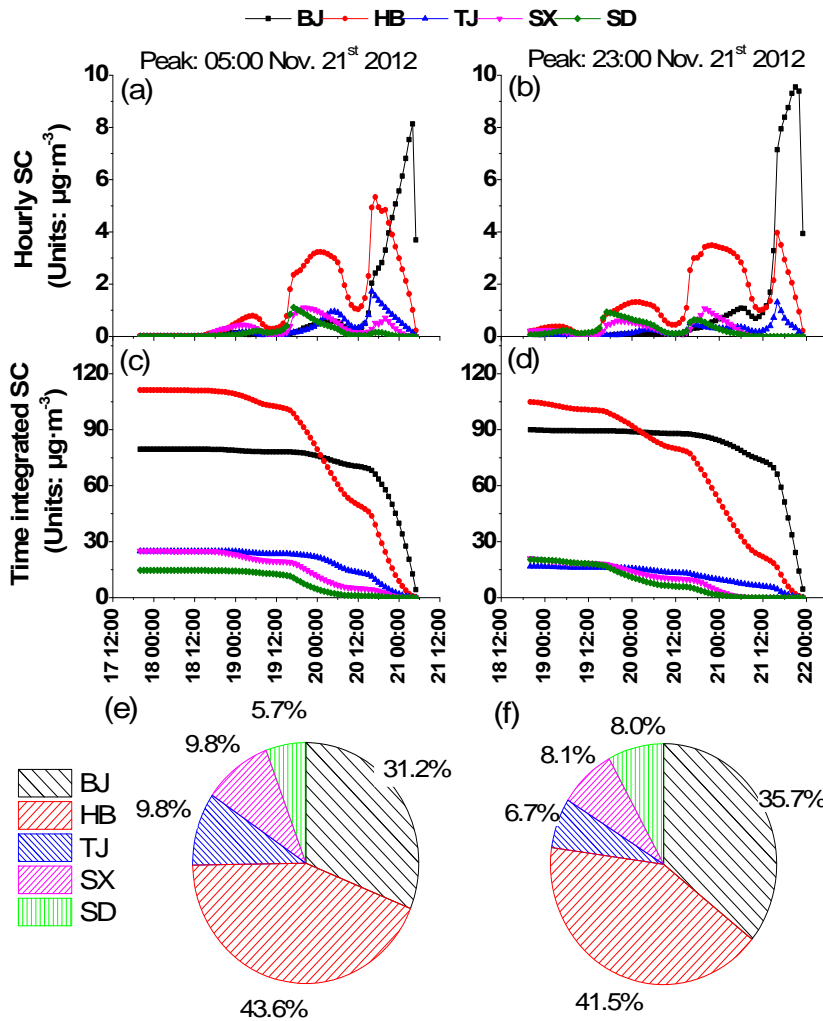
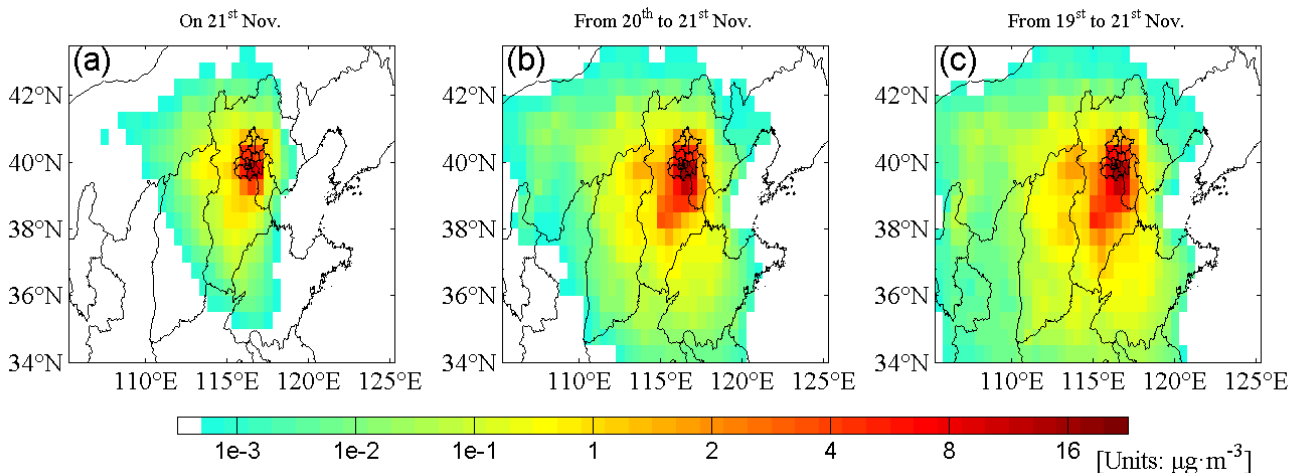


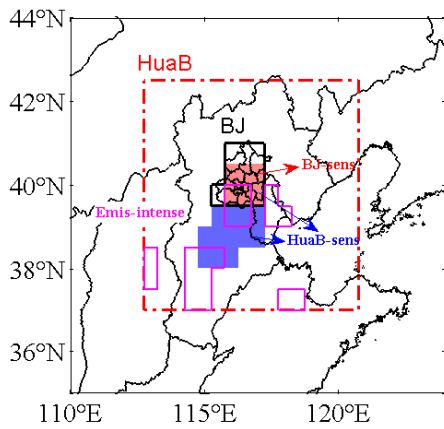
Figure 8. Hourly variations of surface  $PM_{2.5}$  concentrations in Beijing and sensitivity coefficients of surface  $PM_{2.5}$  concentration peaks in Beijing to local and surrounding primary emission sources. The left and right panels correspond to  $PM_{2.5}$  concentration peaks at 05:00 LT and at 23:00 LT on 21 November 2012 respectively. (a–b) illustrate hourly variations of Beijing  $PM_{2.5}$  concentration (black solid dot-line) and hourly instantaneously sensitivity coefficients to local (red closed squares) and surrounding (red open squares) emission sources. (c–d) show the time-integrated sensitivity coefficients to local (red closed squares) and surrounding (red open squares) emission sources.



**Figure 9.** Sensitivity coefficients of surface  $PM_{2.5}$  concentration peaks in Beijing to primary emission sources from local Beijing and each of the surrounding provinces. The left and right panels correspond to  $PM_{2.5}$  concentration peaks at 05:00 LT and at 23:00 LT on 21 November 2012 respectively. (a–b) illustrate hourly instantaneous sensitivity coefficients to emission sources from local Beijing, Hebei province, Tianjin city, Shanxi province and Shandong province. (c–d) show the time-integrated sensitivity coefficients to local and surrounding provincial emission sources. (e–f) are the contribution ratios of emission sources from each surrounding province to  $PM_{2.5}$  concentration peaks.



**Figure 10.** 24-h (a), 48-h (b) and 72-h (c) integrated sensitivity coefficients of surface  $PM_{2.5}$  concentrations to primary emission sources in Beijing on 21 November 2012.



Regions	Number of grid cells	Sensitive area ratios (%)
HuaB-sens	18	10.2
HuaB	176	
BJ-sens	6	60.0
BJ	10	
Emis-intense	18	10.2

**Figure 11. Domain definition of Huabei (HuaB, in red dot-dashed frame), Beijing (BJ, in black solid frame), sensitive Beijing (BJ-sens, red shaded), sensitive Huabei (HuaB-sens, red shaded and blue shaded) and emission intensive (Emis-intense, in pink solid frame) regions.**

**Notes:** HuaB-sens area ratio = 'HuaB-sens floor space'/'HuaB floor space'×100%;

**BJ-sens area ratio** = 'BJ-sens floor space'/'BJ floor space'×100%;

**Emis-intense area ratio** = 'Emis-intense floor space'/'HuaB floor space'×100%.